AD-A139 359 AN INVESTIGATION OF THE STRUCTURE AND HIGH TEMPERATURE 1/1
MECHANICAL PROPERT.. (U) STANFORD UNIV CA DEPT OF
MATERIALS SCIENCE AND ENGINEERING W D NIX FEB 84
UNCLASSIFIED AFOSR-TR-84-0163 AFOSR-81-0022 F/G 11/6 NL

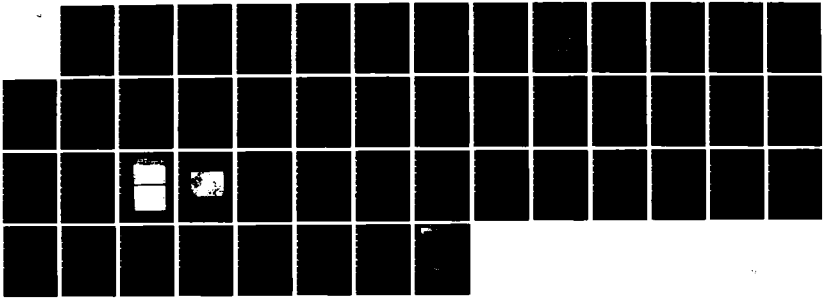

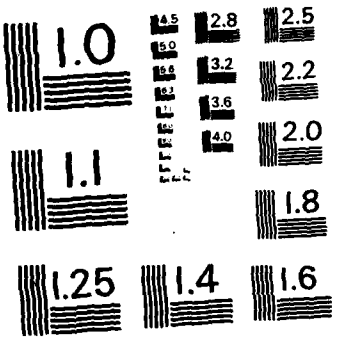

INTERIM SCIENTIFIC REPORT

(For the period 1 October 1982 to 30 September 1983)

AN INVESTIGATION OF THE STRUCTURE AND HIGH TEMPERATURE MECHANICAL PROPERTIES OF OXIDE DISPERSION STRENGTHENED ALLOYS

Submitted to

Department of the Air Force
Directorate of Electronic and Solid State Sciences
Air Force Office of Scientific Research
Bolling AFB, Building 410, Washington, D.C. 20332
Attn: Dr. Alan H. Rosenstein

Submitted by

Professor William D. Nix (Principal Investigator)
Department of Materials Science and Engineering
Stanford University, Stanford, California 94305

February, 1984

This research was supported by the Air Force Office of Scientific Research (AFOSC) under Grant No. AFOSR-81 - 0022

Approved for public release; distribution unlimited

Qualified requesters may obtain additional copies from the Defense Documentation Center; all others should apply to the Clearing House for Federal Scientific and Technical Information

SECURITY CLASSIFICATION OF THIS PAGE (When Data Entered)

REPORT DOCUMENTATION PAGE	READ INSTRUCTIONS BEFORE COMPLETING FORM
1. REPORT NUMBER: AFOSR-TR- 84-0168	2. GOVT ACCESSION NO. AD-A139 359 / 3. RECIPIENT'S CATALOG NUMBER
4. TITLE (and Subtitle): An Investigation of the Structure and High Temperature Mechanical Properties of Oxide Dispersion Strengthened Alloys	5. TYPE OF REPORT & PERIOD COVERED: Interim Scientific Report 6. PERFORMING ORG. REPORT NUMBER
7. AUTHOR(s): William D. Nix, Professor	8. CONTRACT OR GRANT NUMBER(s): AFOSR-81-0022
9. PERFORMING ORGANIZATION NAME AND ADDRESS: Department of Materials Science & Engineering Stanford University Stanford, California 94305	10. PROGRAM ELEMENT, PROJECT, TASK AREA & WORK UNIT NUMBERS: 61102F 2306/A1
11. CONTROLLING OFFICE NAME AND ADDRESS: Air Force Office of Scientific Research (NE) Bolling AFB, Building 410 Washington, D.C. 20332	12. REPORT DATE: Feb. 84 13. NUMBER OF PAGES: 38
14. MONITORING AGENCY NAME & ADDRESS(if different from Controlling Office)	15. SECURITY CLASS. (of this report) 15a. DECLASSIFICATION/DOWNGRADING SCHEDULE

16. DISTRIBUTION STATEMENT (of this Report)

Approved for public release;
distribution unlimited.

17. DISTRIBUTION STATEMENT (of the abstract entered in Block 20, if different from Report)

18. SUPPLEMENTARY NOTES

19. KEY WORDS (Continue on reverse side if necessary and identify by block number)

Oxide dispersion strengthened metals, solute strengthening, dispersion strengthening, ODS superalloys, superplasticity, creep strength.

20. ABSTRACT (Continue on reverse side if necessary and identify by block number)

The structure and high temperature mechanical properties of oxide dispersion strengthened alloys are being studied. We have observed and studied superplastic properties in fine grained MA 6000 and MA 754. These properties have been described by a model which couples dislocation and diffusional creep. The creep properties of coarse grained MA 754 are also being studied. We have observed that cavitation contributes to the creep rate at low stresses and high temperatures and that grain boundary degradation occurs by diffusional processes. Work on the structure and properties of Al-Fe-Ce alloys is just starting.

DD FORM 1 JAN 73 1473 EDITION OF 1 NOV 65 IS OBSOLETE

UNCLASSIFIED

SECURITY CLASSIFICATION OF THIS PAGE (When Data Entered)

TABLE OF CONTENTS

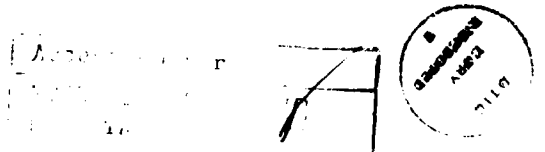

A-1

I. SUMMARY OF RESEARCH

The overall objective of this research has been to develop a better understanding of the structure and high temperature mechanical properties of oxide dispersion strengthened metals. In this report we describe some of the progress we have made during the past year.

Our work on the superplastic properties of ultra-fine-grained ODS alloys was completed during the past year. This work was highlighted in our last Interim Progress Report and is described in a forthcoming publication. Thus, it will not be described in this report. It may be of interest to note that J. K. Gregory's Ph.D. dissertation on this subject has been used by INCO to guide the development of a die forging process for ODS superalloys.

Much of our work during the past year has focused on the high temperature creep and fracture properties of coarse grained MA 754. This alloy is currently being used in gas turbine engines and its mechanical properties at very high temperatures are of great interest. We have conducted constant stress creep tests at temperatures ranging from 1000 to 1200°C at strain rates as low as 10^{-9} s^{-1}. This study has revealed a new mechanism of creep and fracture at very low stresses and strain rates. This process involves cavitation of transverse grain boundaries and leads to intergranular fracture. The creep rates in this low stress regime are greater, by many orders of magnitude, than the expected creep rates based on extrapolation of high stress data. This observation is significant because it indicates that this alloy is not nearly as creep resistant at very high temperatures and low stresses as might be expected from other data. Our study of two different heats of MA 754 suggests that the low stress creep process can be influenced by the grain morphology. This, in turn, may provide a means for

for controlling this low stress creep process.

The results obtained during the past year were made possible by the development and use of several different new experimental techniques. A special tantalum extensometer installed in the high temperature creep apparatus permitted the measurement of strain rates below 10^{-9} s^{-1}. The low stress creep regime could not have been studied without this equipment. In addition, we made use of the technique of small angle x-ray scattering to determine, for the first time, the distribution of dispersoid sizes in MA 754. This has permitted us to understand the difference in strength properties of the two heats. Also, newly developed pole figure facilities at Stanford were used to fully document the crystallographic texture of the two heats of MA 754.

Our study of the structure and mechanical properties of Al-Fe-Ce alloys has continued during the past year. We have compared the high temperature flow properties of this alloy with those for ODS - Al made by mechanical alloying. At temperatures below 400°C the Al-Fe-Ce is substantially stronger than the ODS-Al. The higher volume fraction of dispersoid in the Al-Fe-Ce is responsible for this difference. However, at 500°C the Al-Fe-Ce alloy loses much of its strength compared to ODS-Al. This loss of strength is not due to coarsening of the microstructure as annealing the alloy at 500°C for long periods of time does not reduce its strength at lower temperatures. These results indicate that oxide strengthening is superior to strengthening by intermetallic phases at very high temperatures. It suggests that the high temperature mechanical properties of Al-Fe-Ce alloys might be improved significantly by mechanical alloying.

Our work on the flow properties of ultra-fine grained ODS alloys has raised fundamental questions about the nature of superplastic flow . In particular, our studies have shown an extended regime of deformation at strain rates less than the optimum strain rate for superplasticity. Diffusional creep appears to be inhibited in this regime for reasons that are still unknown. Our understanding of this problem and of superplasticity in general is reviewed in a recent paper on this subject; this appears as an Appendix in this report.

A. High Temperature Creep of Coarse Grained MA 754

Oxide dispersion strengthened (ODS) nickel based alloys owe their high temperature strength to the presence of inert oxide particles, which inhibit dislocation motion. A second requirement for optimizing creep resistance is an elongated grain structure. In mechanically alloyed ODS alloys such as MA 754, a coarse, elongated grain structure can be formed by extensive thermomechanical processing. During the past year we have investigated the effect of variation in grain structure on the creep properties of MA 754 at 1000°C and above. A dramatic change in the stress exponent at low applied stresses is observed as the grain morphology is changed.

1. Variations in Grain Morphology

The overall grain morphologies of the two MA 754 heats investigated are shown in Figure 1. Heat 1, Figure 1(a), consists of coarse, fiber-shaped grains of relatively uniform size. The longitudinal and transverse grain boundaries in this heat are fairly smooth. In contrast, the grain morphology of Heat 2, Figure 1(b), consists of a duplex grain structure: coarse, recrystallized grains are

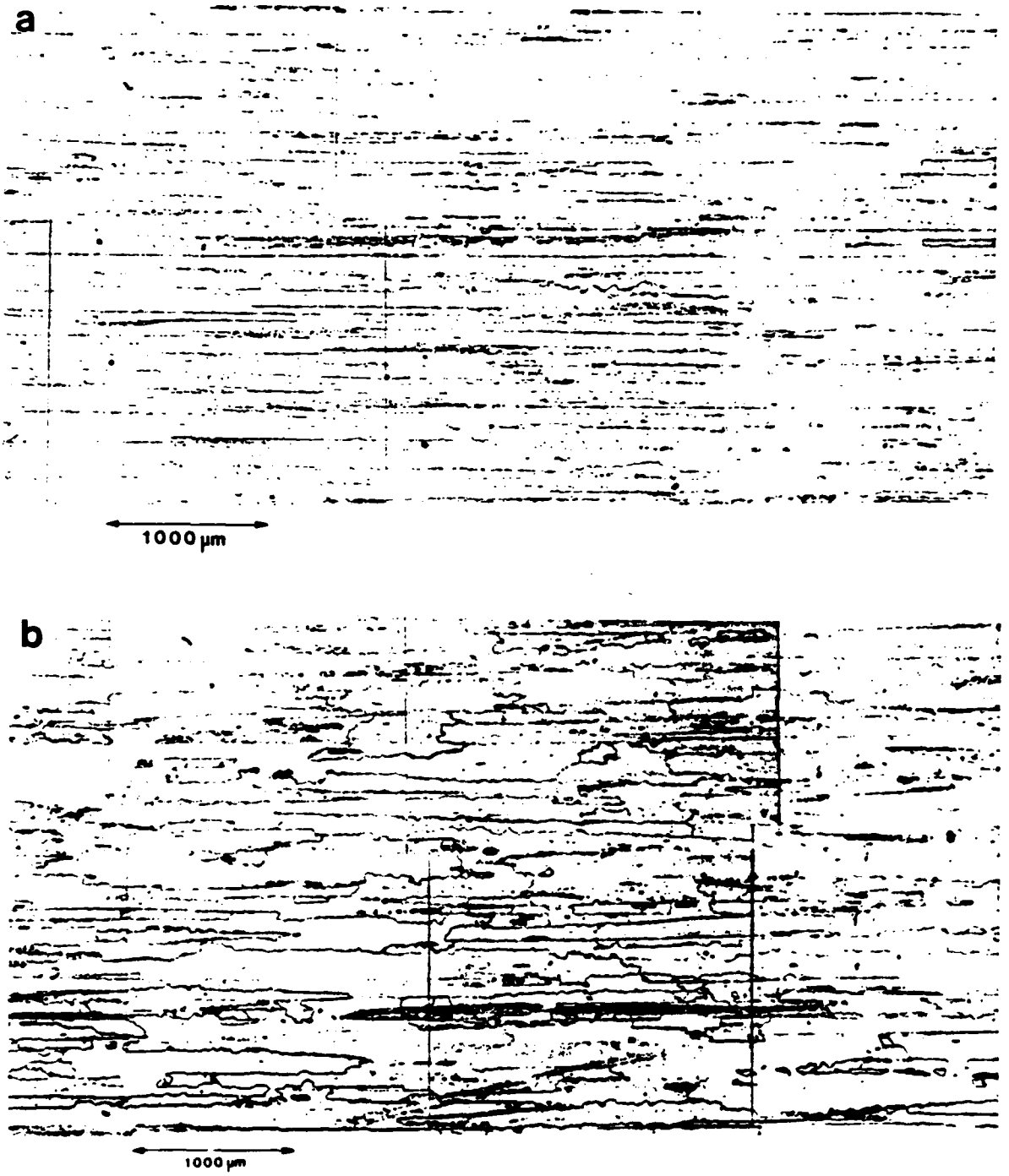

Figure 1: Extrusion plane views of the coarse-grained MA 754 Heats Investigated. Longitudinal direction is horizontal, long transverse is vertical. (a) Heat 1 (Heat #DTO6A7B), (b) Heat 2 (Heat #DT15A5B1-1).

found, along with pockets of fine, equiaxed grains in the size range of 5-20 μm. These fine, equiaxed grains occupy approximately 2% areal fraction in the extrusion plane. Close inspection of Figure 1(a) also reveals some fine equiaxed grains in Heat 1, but they are isolated grains and approximately 1/10 the areal fraction found in Heat 2. The grain aspect ratios (GAR's) were measured for Heats 1 and 2 by means of a line intercept technique: the GAR's are 7.2 and 5.9, respectively. The measured intercepts are summarized in Table I. It should be emphasized that the sampling method used to determine the intercepts leads to an intercept length in the longitudinal direction which counts very few equiaxed grains.

Pole figures of the two heats have been generated in reflection and are shown in figures 2 and 3. Both heats' pole figures indicate a strong {110}<001> "cube on edge" texture. Both Figures 2(d) and 3(d) indicate that the longitudinal direction is within 6 degrees of <001> in both heats. Comparison of figures 2(b) and 3(b) indicate that there is a slightly larger deviation of extrusion plane normals from <110> in Heat 2. This macroscopic observation of a stronger {110} texture in Heat 1 is supported by selected area diffraction in the electron microscope: Heat 1 specimens cut from the extrusion plane contain grains which are extremely close to the (110) zone axis. Most of the grains from extrusion plane specimens of Heat 2 are close to the (110) zone axis, but a few are observed to be

TABLE I: Calculation of Grain Aspect Ratio for Coarse-Grained MA 754

	Intercept Length, μm			
	Longitudinal	Long Transverse	Short Transverse	GAR
Heat 1	714	131	75	7.2
Heat 2*	550	156	56	5.9

* Measurement does not include fine pockets of equiaxed grains found in this heat

closer to the (013) zone axis. The fine, equiaxed grains in Heat 2 are expected to have random orientation - they occupy such a small volume fraction that a macroscopic pole figure experiment cannot reveal their texture.

2. Creep Testing of MA 754

The fabrication and installation of a Tantalum extensometer during the last year has allow us to extend our strain rate measurements to as low as 10^{-10} (sec^{-1}) without the need for temperature-co.r .sating the displacement data. This capability has proven essential for measuring stress exponents at the lower stresses where cavitation occurs.

The constant stress-minimum strain rate data for the pure fiber (Heat 1) grain morphology at 1200°C is shown in Figure 4(a). At high stresses, a stress exponent of 46 is measured, and fracture is transgranular. At stresses below 103 MPa the stress exponent, n, abruptly decreases to a value of 5 and intergranular fracture is observed. The <001> single crystal TD NiCr data of Lund (1) is shown for comparison in Figure 4(a). The n value measured for MA 754 is approximately equal to that of single crystal TD NiCr - implying that the high stress regime in MA 754 is basically single crystal behavior. At the high strain rates dislocation creep proceeds within the grains, and there is insufficient time for cavitation to take place.

The minimum strain rate-stress data for the duplex grain morphology (Heat 2) at 1200 °C is shown in Figure 4(b). The data lines for Heat 1 are included in this figure for comparison. As with the pure fiber morphology, two stress exponent regimes are observed. At the high stresses, a stress exponent of 35 is measured, while at lower stresses an n value of 2 is found. Note that in contrast to the pure fiber grain morphology, the transition in stress exponents is quite gradual. At the highest stresses, Monkman-Grant constants, C_{M-G}, of 2.4×10^{-2} are measured, and C_{M-G} decreases to approximately $5. \times 10^{-3}$ at the lower stresses. This decline in C_{M-G} is indicative of a transition from transgranular to intergranular fracture, and is identical in behavior with the trends observed in the pure fiber grain morphology.

The 1093 °C minimum strain rate-stress data is shown in Figure 5. Figure 5(a) indicates that the pure fiber morphology has an n value of 42 at high sresses and n declines to 16 at stresses below 122 MPa. As at 1200°C, the high stress exponent regime is similar to single crystal behavior with transgranular fracture, while cavitation and intergranular fracture is observed in the low stress regime. Figure 5(b) shows the data for the duplex grain morphology at 1093 °C: again, two distinct deformation regions are observed. It is important to note that the n value for the duplex grain morphology is equal to 2 at both 1200 °C and 1093°C. By comparison, the low stress n for the pure fiber

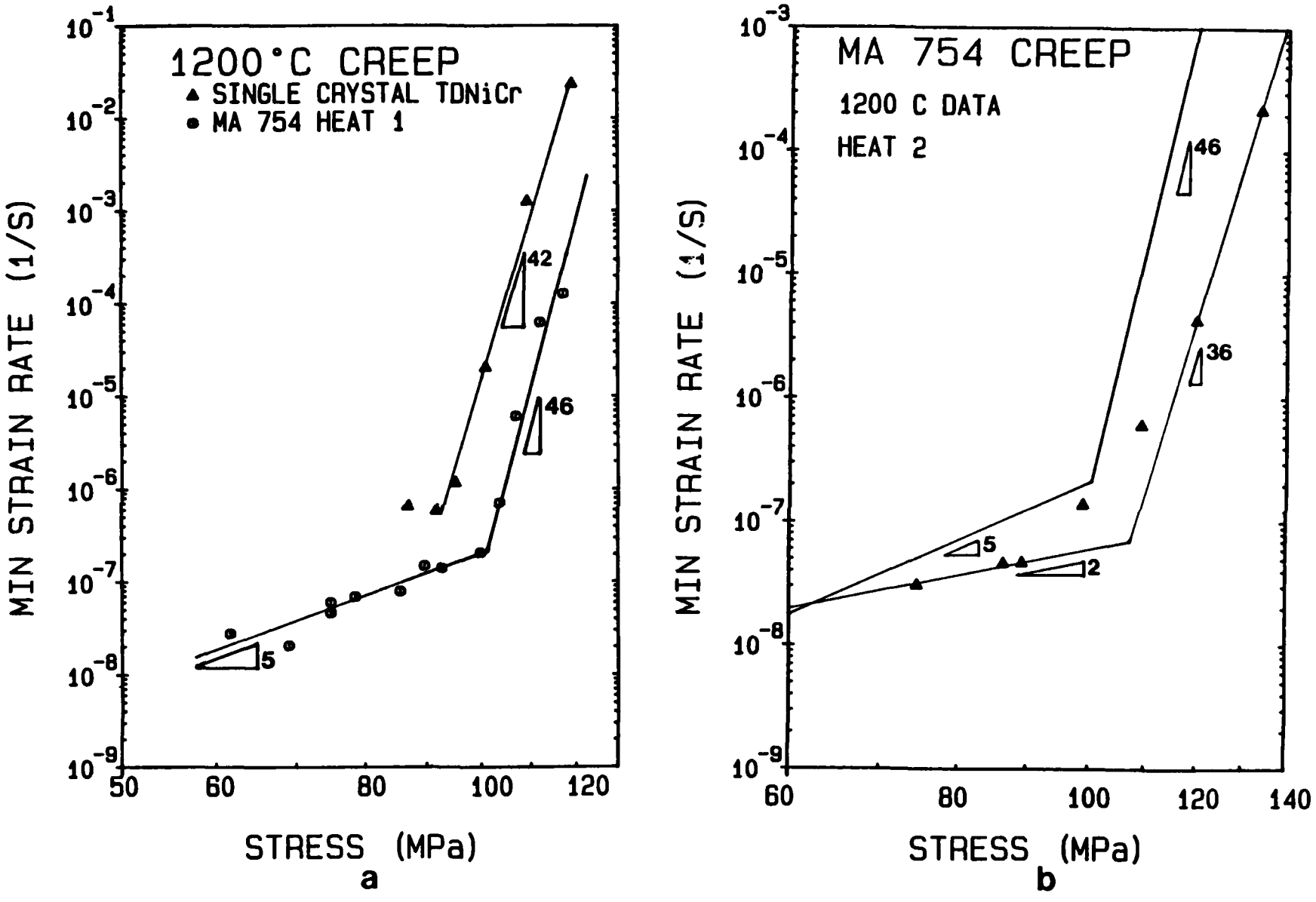

Figure 4: Constant Stress Creep data for MA 754 at 1200°C: (a) Heat 1, with single crystal TDNiCr data of Lund for comparison, (b) Heat 2, with data lines of Heat 1 included for comparison.

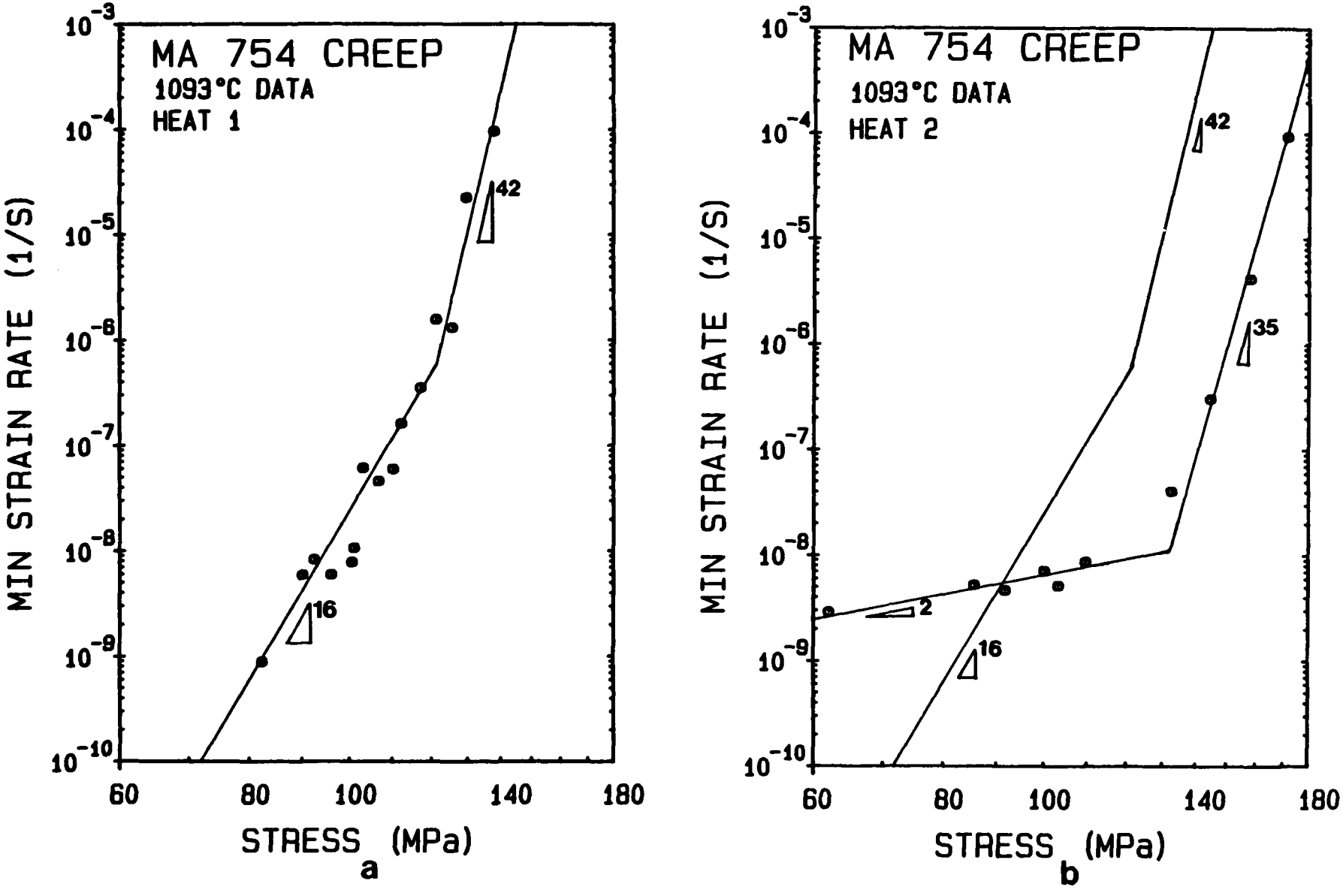

Figure 5: Constant Stress Creep data for MA 754 at 1093°C: (a) Heat 1, (b) Heat 2, with data lines of Heat 1 included for comparison.

morphology is only 5 at 1200°C, but increases to 16 at 1093 °C. Note that below 90 MPa the pure fiber grain morphology has a slower strain rate than the duplex grain morphology, whereas the duplex grain morphology is stronger above 90 MPa. This implies that the cavitation rate is a much stronger function of stress for the pure fiber grain morphology; while cavitation in the duplex grain morphology has a weaker stress dependence and is thus more cavitation resistant in the stress range from 90 MPa up to about 128 MPa.

The creep data at 1000°C, shown in Figure 6, is very similar to the 1093 °C data in overall behavior. The n values for the pure fiber mophology, shown in Figure 6(a), are 40 and 14 at the high and low stresses, respectively. As at the higher temperatures, transgranular fracture is observed at the higher stresses, while cavitation and subsequent intergranular fracture is observed at the low stresses. The <001> single crystal TD NiCr data of Lund (1) in Figure 6(a) again indicate that the high stress regime is basically single crystal behavior. For the duplex grain morphology, shown in Figure 6(b), only one stress exponent, n=30, is measured. It is suspected that the low stress exponent regime will be reached at strain rates in the 10^{-10} (sec^{-1}) range.

3. High Stress Exponent Regime.

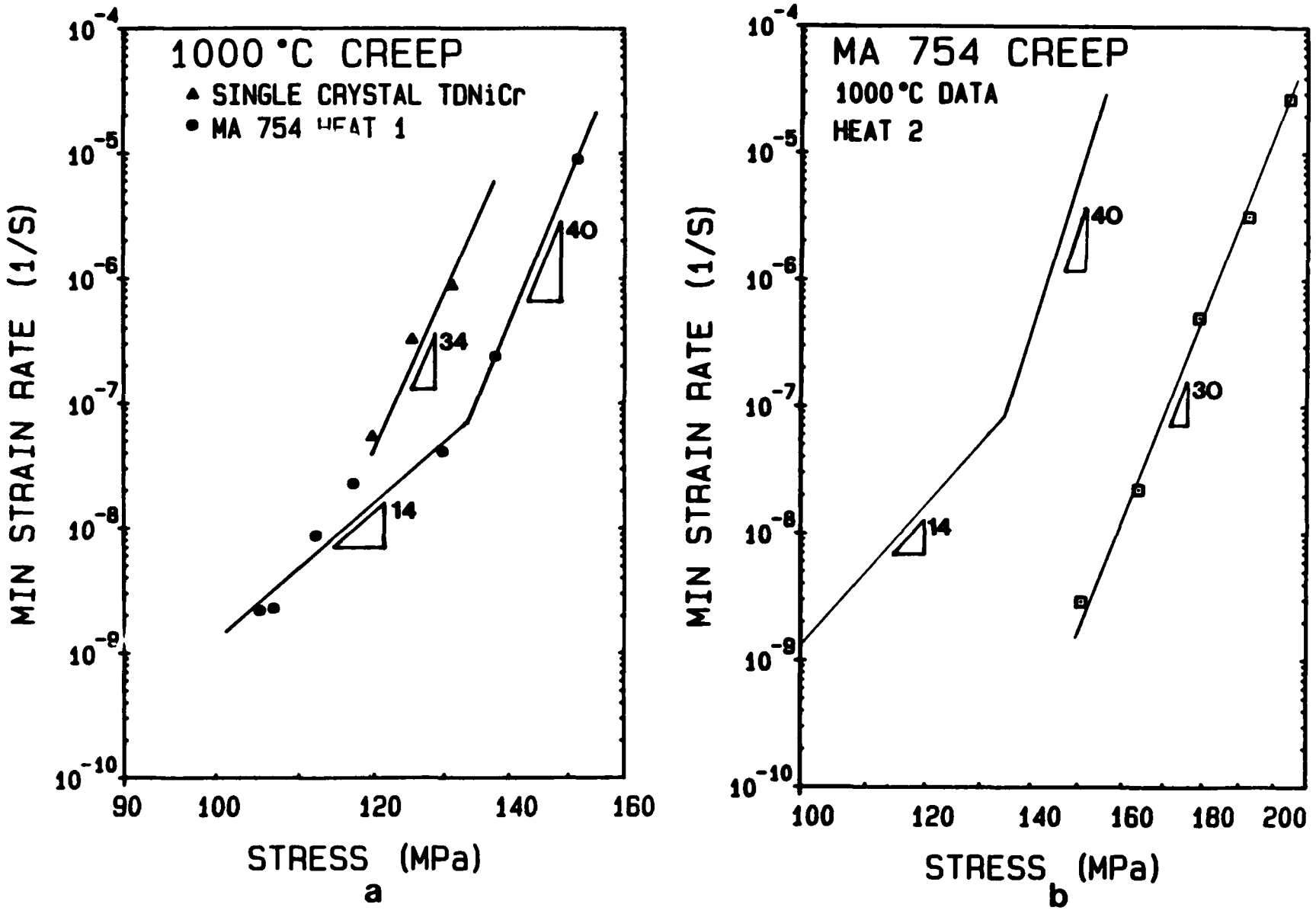

Figure 6: Constant Stress Creep data for MA 754 at 1000°C, (a) Heat 1, with single crystal TDNiCr data of Lund for comparison, (b) Heat 2, with data lines of Heat 1 included for comparison.

Inspection of Figures 4,5, and 6 shows that Heat 2 is significantly stronger than Heat 1 at the high stresses where dislocation creep is proceeding within the grains and fracture is transgranular. In Table II we have listed the stress necessary to generate a minimum strain rate of 10 (sec^{-1}) as a function of temperature for both heats, and it can be seen that Heat 2 is stronger than Heat 1 by differences of 14, 23 and 24 % in stress at 1200, 1093 and 1000°C respectively. Since the deformation behavior in this regime is similar to single crystal behavior, it is thus expected that the Orowan stress,

$$\sigma_{Orowan} = \frac{0.84\ \mu b}{\bar{L}}$$

where μ is the shear modulus, b is the burgers vector of the dislocation, and $\bar{L}$ is the average planar dispersoid separation distance, should apply. Since Heat 2 exhibits higher strength in the single crystal regime, $\bar{L}$ in Heat 2 should be smaller than in Heat 1.

The average planar dispersoid separation distance, $\bar{L}$, can be calculated for an ODS alloy if one can measure the size distribution and volume fraction of dispersoids. Thus, $\bar{L}$ is given by the following relations (2):

$$\bar{L} = d - 2r_{av}$$

$$d = \left[\frac{8}{3\sum_i f_i / r_{vi}^2} \right]^{1/2}$$

TABLE II. High Stress Regime, MA 754 Strength Differences

Stress to Generate $\dot{\varepsilon}_{MIN} = 1 \times 10^{-5}$ (sec^{-1})			
Temperature	Heat 1	Heat 2	% Difference
1200°C	108 MPa	123 MPa	14%
1093°C	130 MPa	160 MPa	23%
1000°C	152 MPa	188 MPa	24%

where r_{av} is the average dispersoid diameter, d is the mean planar center to center dispersoid spacing, f_i is the volume fraction of the i size class of particles with an average radius r_{vi}. Thus, f_i, r_{av}, and r_{vi} are obtained from a measurement of the dispersoid size distribution and volume fraction of dispersoids in a given ODS alloy.

Previous investigations of creep in ODS alloys have relied upon electron microscopy to measure the particle size distribution and chemical analysis to obtain the dispersoid volume fraction. A major problem with such TEM investigations is that a small volume is sampled and only about 10^3 diameters are measured to give the size distribution. During the past year we have performed a series of Small Angle X-Ray Scattering (SAXS) experiments in collaboration with Dr. Steven Spooner of Oak Ridge National Laboratory in order to determine dispersoid size distributions in MA 754. The major advantage of the SAXS technique is that the volumes sampled are about 10^6 times larger than in the TEM experiment - each SAXS scattering spectrum contains size information from approximately 10^9 particles. A particle of a given radius r scatters with a characteristic intensity as a function of angle ($I(r,\Theta)$), therefore, the scattering spectrum is treated as the superposition of scattering from individual particles. Dispersoid size distributions are then extracted by two different methods. The simplest method consists of calculating the log-normal distribution parameters from the

scattering data using a method based on the analysis of Harkness, et. al. (3). The second method - which does not assume a functional form of the distribution - consists of an integral transform technique first used by Brill, et. al. (4).

Preliminary results of the two methods to extract dispersoid size distributions from the scattering spectra indicate that the value of $\overline{L}$ is approximately 25% smaller in Heat 2 than Heat 1. This agrees well with the observed differece in creep strength at high stresses observed in the two heats. These results confirm that the high stress exponent regime for MA 754 is single crystal behavior, ie, the difference in strength depends upon the average spacing of dislocation obstacles. A companion TEM investigation of dispersoid size distributions is nearing completion, and we will then be able to compare the results of two independent methods of determining dispersoid size distributions and volume fractions in ODS alloys.

4. Low Stress Exponent Regime.

The stress exponents measured for the two different heats of MA 754 at low stresses are observed to be quite different. The n values for Heat 1 were found to be 5, 16 and 14 for 1200, 1093 and 1000 °C respectively, while n values of 2 were measured at 1200 and 1000°C for Heat 2. These results suggest that the processes governing creep deformation behavior at low stresses in MA 754 depend

strongly on the grain morphology. Thus, Heat 1 with a pure fiber grain morphology exhibits n values significantly higher than Heat 2 with a duplex grain morphology. It should be noted that the difference in GAR between these two heats cannot explain the large difference in measured stress exponents.

It is essential that any deformation model of low strain rate creep behavior of MA 754 account for the observed cavitation of the transverse grain boundaries. As described in the previous progress report, during the course of low strain rate creep in MA 754 cavities are observed on the transverse grain boundaries and intergranular fracture occurs by means of their subsequent growth and interlinkage. We have observed small, dispersoid-free zone formation adjacent to these cavities, suggesting that these cavities grow by means of plating metal atoms onto the adjacent grain boundary regions. Since compatibility with adjoining grains must be maintained during this cavity growth, it is apparent that the growth of these cavities is constrained by either the deformation or relative motion of adjoining grains.

As the transverse grain boundary cavities grow, their ability to sustain normal tractions is diminished, and load is shed onto adjacent grains. This load shedding gradually increases the stress within the adjacent grains, where deformation is governed by the high stress exponent ($n \simeq 40$), single crystal behavior. For a given applied stress, there

is a critical amount of load shedding which can take place beore dislocation creep in adjoining grains becomes very rapid. Once this point is reached fracture proceeds very quickly.

The deformation process which constrains the cavity growth in MA 754 determines the value of n at low stresses. It appears that in the case of the duplex grain morphology encountered in Heat 2, the presence of pockets of fine grains in the longitudinal grain boundaries allows for relative motion of adjoining large grains to occur by means of grain boundary sliding of the fine grains. This accounts for stress exponent values of 2 measured for Heat 2 at 1093 and 1200 C. On the other hand, in Heat 1 no pockets of fine grains are found. Cavitation in this case must be constrained by the power law creep of the adjoining grains. This leads to the high stress exponents measured in Heat 1.

The concept of constrained cavity growth was first proposed by Dyson (5) in an attempt to model the cavitation process in engineering alloys where cavities are found on isolated grain boundary facets. A subsequent analysis by Raj and Ghosh (6) has modeled the case of cavity growth constrained by power law creep of adjoining grains. In the near future, we will apply the analysis of Raj and Ghosh to the case of constrained cavity growth in Heat 1 where power law creep of adjacent grains apparently compensates for the grain boundary separation caused by cavity growth. We will

then consider the appropriate case for Heat 2, ie, constrained cavity growth compensated by grain boundary sliding of pockets of fine grains.

B. Structure and Properties of Al-Fe-Ce Alloys

1. Compression Tests of Rapidly Solidified Al-8.0Fe-3.4Ce

During the past year, we have initiated a study of the high temperature flow properties of Al-Fe-Ce alloys. Specifically, the material currently under investigation is an extrusion of rapidly solidified Al-8.0Fe-3.4Ce. Constant true strain compression tests have been performed on this material using our recently installed Instron electro-mechanical testing machine in conjunction with a Hewlett-Packard 3054A data acquisition and control system. Compression tests have been conducted at temperatures ranging from 523 to 773 K and at strain rates varying from 10^{-6} to 10^{-3} s^{-1}. It should be noted that prior to testing, each sample was subjected to a one hour stabilizing treatment at 650 K.

The results of the constant true strain rate compression tests are shown in Figure 7. From this figure it is readily apparent that rapidly solidified Al-8.0Fe-3.4Ce is considerably stronger than oxide dispersion strengthened (ODS) aluminum over a fairly wide range of temperatures and strain rates. In addition Al-8.0Fe-3.4Ce, at temperatures below 623 K, exhibits a fairly large stress exponent, on the order of 8 to 24. Unfortunately however Al-8.0Fe-3.4Ce, unlike ODS aluminum, undergoes considerable softening when tested at high temperatures and/or low strain rates. As can be seen in Figure 7, Al-8.0Fe-3.4Ce tested at 773 K and at a strain rate of 10^{-5} s^{-1} is noticeably softer than similarly tested ODS aluminum. It is interesting to note that this softening behavior is not simply a result of particle coarsening due to long time elevated temperature exposure. From Figure 7

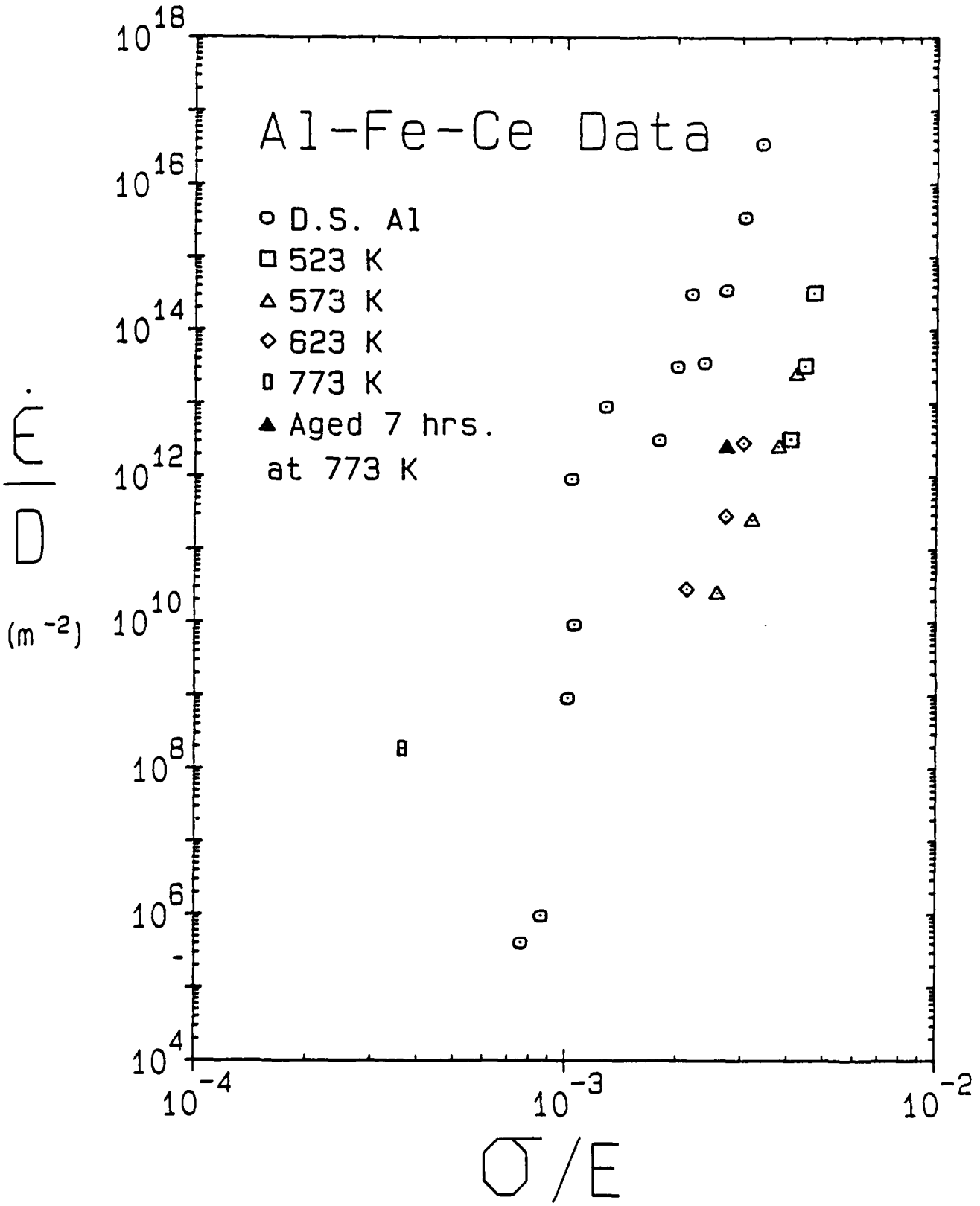

Figure 7: Temperature compensated steady state strain rate versus modulus compensated steady state stress for Al-8.0 Fe-3.4 Ce. Filled symbol indicates sample was aged 7 hrs at 773K prior to testing. D.S. aluminum data is included for comparison (Ref. 1).

it can be seen that aging at 773 K for seven hours prior to testing at 573 K and at a strain rate of 10^{-4} s^{-1} is able to produce significant softening in Al-8.0Fe-3.4Ce. Thus the loss of strength observed in the specimen tested at 773 K must be related to a change in deformation behavior at this temperature and strain rate.

2. TEM Investigation

A number of tested as well as untested samples of Al-8.0Fe-3.4Ce have been examined via transmission electron microscopy. As expected, the grain size is quite fine, approximately 5 μm. A large volume fraction of second phase particles are present, however as shown in Figure 8, these particles are heterogeneously distributed throughout the matrix. Below 623 K, no variation in particle size and/or distribution is observed as a result of testing. As can be seen in Figure 9 the major microstructural change resulting from testing below 623 K is the development of subgrains within regions of low particle density.

3. Future Work

Additional compression tests are needed to fully document the unusual reduction in strength associated with testing at elevated temperatures and/or low strain rates. Furthermore, in order to develop an understanding of this behavior, TEM should be used to compare the microstructure of high temperature tested specimens with the microstructure of untested samples of similar thermal history.

During the past year, preliminary attempts to identify second phase particles within the Al-Fe-Ce alloy have been made via combined

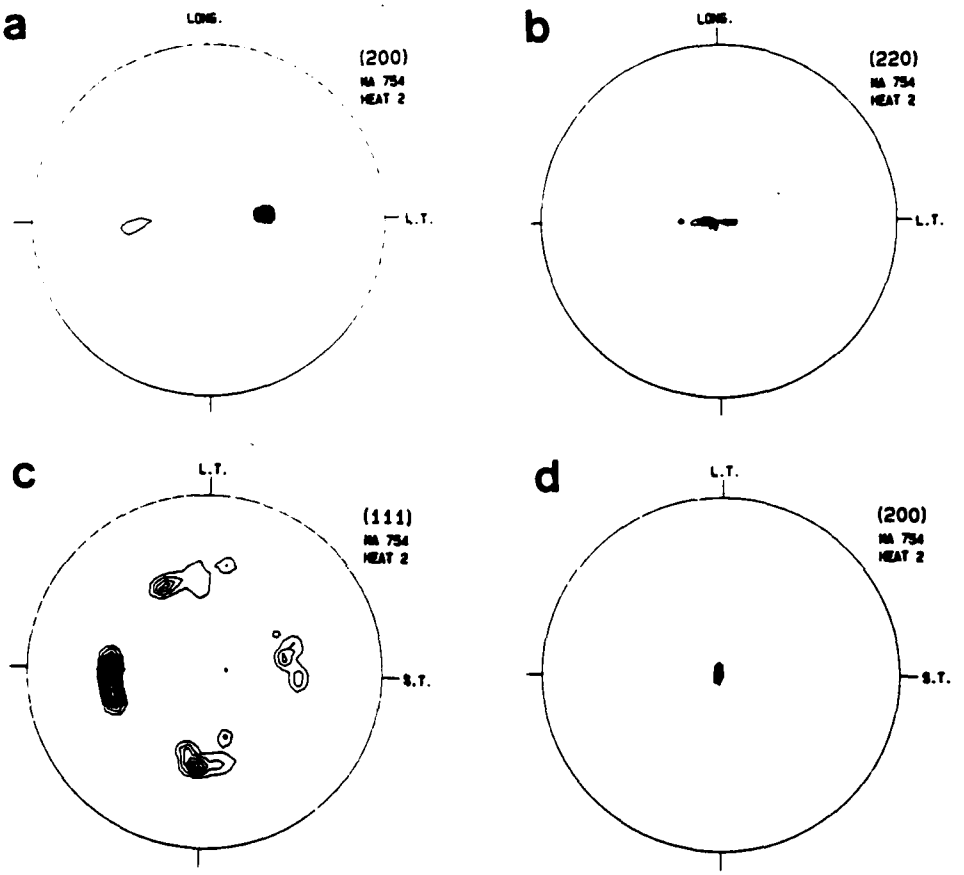

Figure 3: Pole Figures generated in reflection, MA 754 Heat 2, (a) Extrusion Plane, (200) Intensity, (b) Extrusion Plane, (200) Intensity, (c) Transverse Plane, (111) Intensity, (d) Transverse Plane, (200) Intensity.

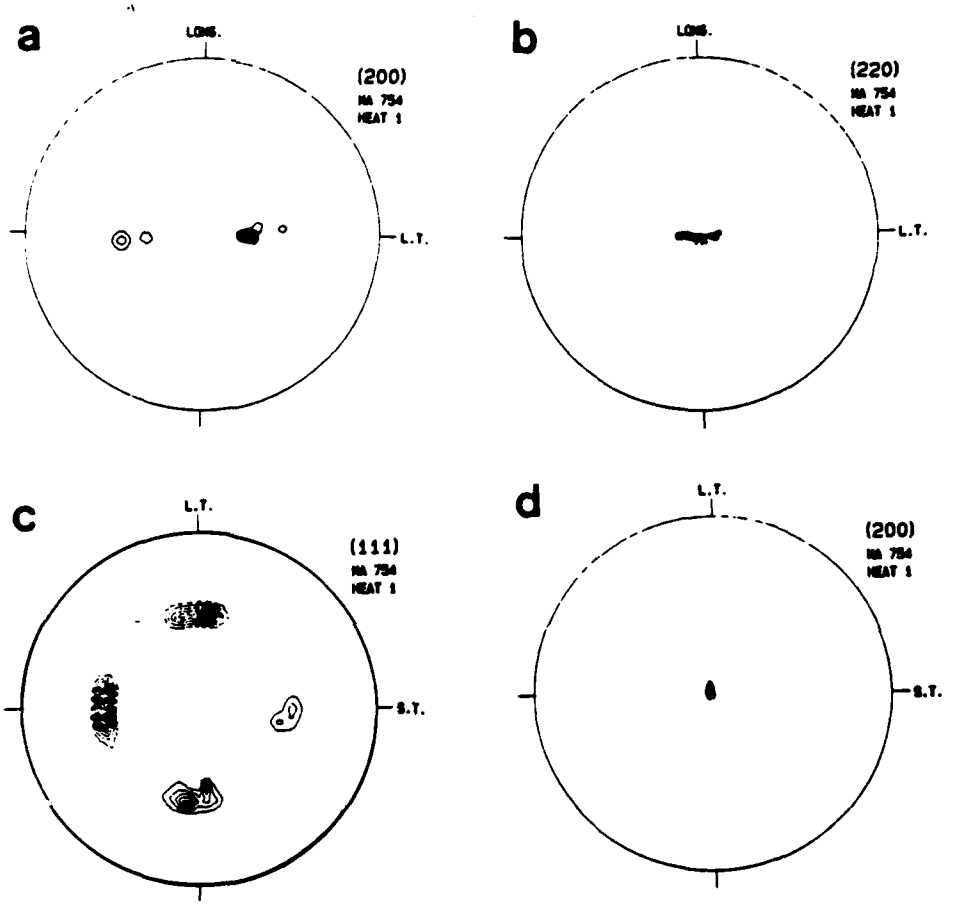

Figure 2: Pole figures generated in reflection, MA 754 Heat 1. (a) Extrusion Plane, (200) Intensity, (b) Extrusion Plane, (200) Intensity, (c) Transverse Plane, (111) Intensity, (d) Transverse Plane, (200) Intensity.

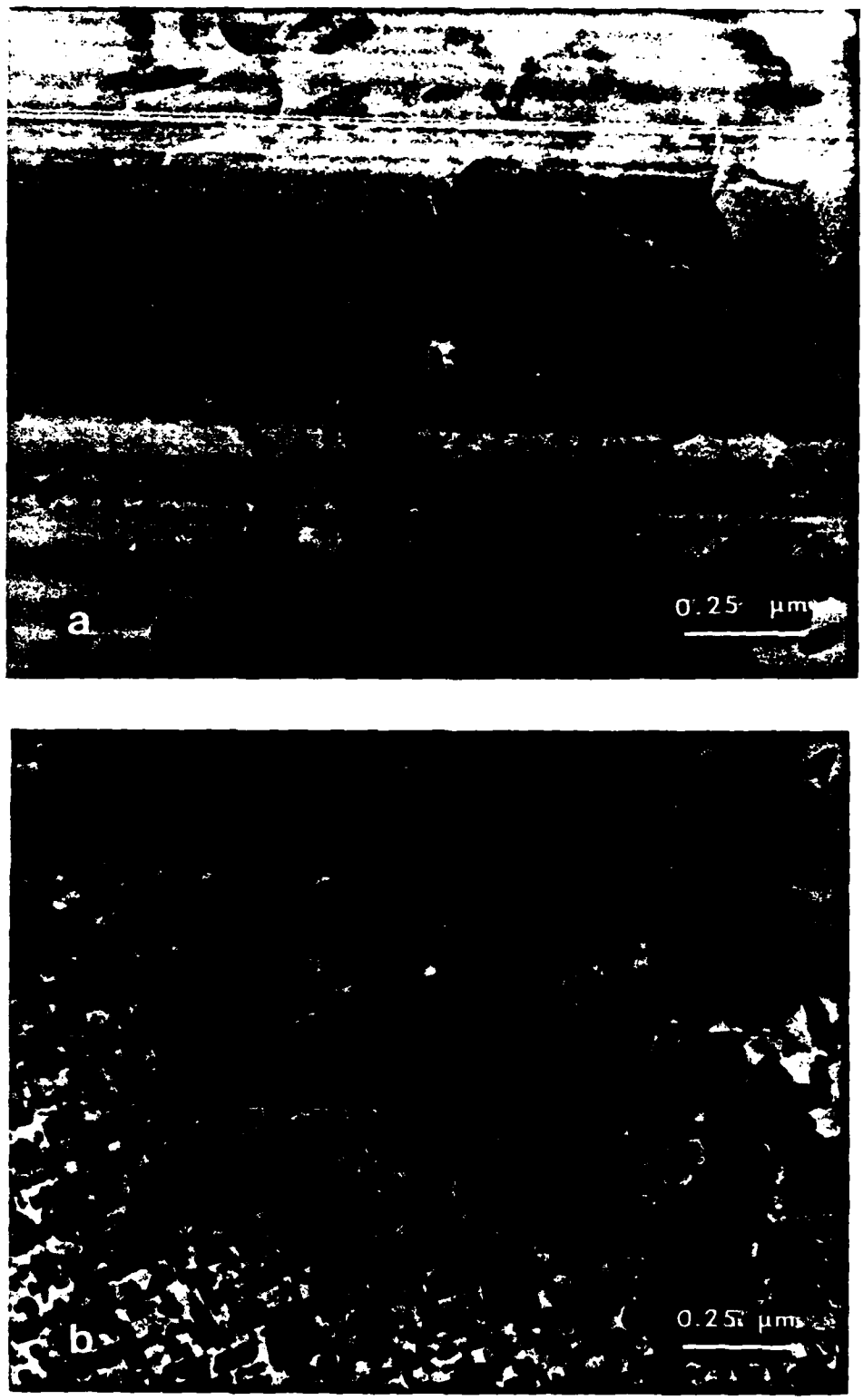

Figure 8: TEM micrograph of untested Al-8.0 Fe-3.4 Ce showing the variation in second phase particle density within the material, (a) low particle density, (b) high particle density.

Figure 9: TEM micrograph of Al-8.0 Fe-3.4 Ce specimen tested at 573 K and at a strain rate of 10^{-5} s^{-1}. 26% strain.

STEM/EDAX techniques. Unfortunately, problems with secondary X-ray flourescence have shown that extraction of particles from the matrix will be required prior to particle identification by energy dispersive X-ray analysis. At this point, our attempts at particle extraction have been unsuccessful however, work is continuing in this area.

REFERENCES

1. R. W. Lund, Ph.D. Dissertation, Stanford University (1975)
2. B. A. Wilcox and A. H. Clauer, Trans. A.I.M.E. 236, 570 (1966)
3. S. D. Harkness, R. W. Gould and J. J. Hren, Philosophical Magazine 19, 115 (1969)
4. O. L. Brill, C. G. Weil, and P. W. Schmidt, J. Colloidal and Interfacial Science 27, 479 (1968)
5. B. F. Dyson, Metal Science 10, 349 (1976)
6. R. Raj and A. K. Ghosh, Met. Trans. 8A, 1291 (1981)
7. W. C. Oliver and W. D. Nix, Acta Metall. 30, 1335 (1982)

C. APPENDIX

ON SOME FUNDAMENTAL ASPECTS OF SUPERPLASTIC FLOW

The principal facts relating to superplastic flow are reviewed in an effort to determine the controlling mechanism. The evidence for grain switching as a flow mechanism is questioned and the associated analysis given by Ashby and Verrall is criticized. It is argued that grain boundary diffusional processes invariably lead to Coble creep and that grain switching, if it does occur, involves extensive grain boundary migration. The observations of grain rotation and changes in crystallographic texture during superplastic flow are analyzed and it is concluded that slip must occur in some of the grains when grain rotations occur. This leads to the conclusion that superplasticity cannot be a purely diffusional process. The sigmoidal stress-strain rate relation found for most superplastic materials is taken as evidence that a separate mechanism for superplastic flow does exist and that the high strain rate sensitivities and high ductilities associated with superplasticity are caused by transitions in flow behavior involving slip and diffusion. The model of Ghosh and Raj is presented as the most attractive description of superplastic flow, but the absence of diffusional creep at low stresses and strain rates remains unexplained.

EXTENSIVE RESEARCH ON superplasticity over the past 15 years has transformed what was once a curious, if not mysterious, phenomenon into a mature subject in mechanical metallurgy. This knowledge in turn has led to a tremendous increase in the number of alloys that can be made superplastic [1-7]. The availability of this ever increasing number of superplastic alloys is expected to produce an even more significant explosion in the applications of superplasticity.

In spite of the rapid progress that has been made, a mechanism of superplasticity has still not been identified. In particular, the exact cause of the high strain rate sensitivity which leads to superplasticity has not yet been found. In the present paper we review some of the evidence that exists regarding the mechanism(s) of superplasticity in an effort to find the controlling mechanism. The viewpoint expressed in this paper is but one of several different approaches to superplasticity. Some comments and criticisms of other conceptions of superplasticity are given but no attempt is made to evaluate all of the other models in a comprehensive way.

We begin the paper with a brief review of some of the basic characteristics of superplastic flow. This is followed by a description of other characteristics which have been widely reported but which have not been decisive factors in determining the controlling mechanism. The evidence for grain switching as a deformation mechanism is questioned and the diffusional analysis of that process is criticized. Special attention is given to grain rotation and the role that slip plays in that process. The rheological properties of superplastic materials are reviewed in an effort to determine if a distinct mechanism of superplasticity exists. This discussion emphasizes the sigmoidal stress-strain rate relationship found for these materials. Finally, a transitional model of superplasticity involving both slip and diffusion is described. The predictions of the model are compared with experiment and some limitations of the model are cited.

CHARACTERISTICS OF SUPERPLASTICITY

Fine grained metallic alloys are said to be superplastic when they exhibit both high elongations and high strain rate sensitivities. Typically the fine grains remain equiaxed in this kind of deformation. These are the basic characteristics of superplastic flow. No single property or feature is sufficient to define superplasticity. For example, metals which have high elongations due to high rates of strain hardening

MICROSTRUCTURAL CONSIDERATIONS

GRAIN SWITCHING - It is well established that grains remain equiaxed during superplastic flow. This fact has led to the view that grains simply rearrange during deformation and retain their overall shape. Support for this concept is found in several different SEM studies of superplastic flow [19-21]. Surface grains are observed to move relative to each other during superplastic deformation suggesting a grain rearrangement deformation process. A limitation of this observation is that interior grains cannot be studied directly. Figure 2 illustrates a hypothetical grain structure in a thin sheet of material which deforms by shear through the plane of the sheet. SEM studies are usually made by observing the surface of the sheet. The figure shows that sliding of grain arrays in the interior of the sample could lead to "surface grains" which are not subjected to the applied stress and would not deform. These grains would act as inert markers on the surface of the sample and would move relative to each other during deformation. This could explain why some grains do not appear to deform in superplastic flow. The figure suggests that a direct observation of the plane containing the shear displacement (perpendicular to the usual viewing direction) could provide more direct information about any grain switching process that might occur. Observing the surface of a round bar during torsion would be one way to accomplish this.

Throughout this discussion we have assumed that grain switching and grain rearrangement occurs during superplastic flow. In the strictest sense this implies that the number of grains remains constant during superplastic flow and that each grain retains its identity throughout the flow process. An alternate possibility is that continuous recrystallization and grain growth occurs, thereby maintaining a fine equiaxed grain structure during deformation.

The possibility that grain switching could occur by diffusional processes was studied by Ashby and Verrall [22] who developed a model based on observations of deformation of an oil emulsion. An oil emulsion consisting of "grains" of oil separated by "grain boundaries" composed of a thin layer of detergent was deformed by extruding a portion of the emulsion through a die between two glass plates. The grains were observed to switch their neighbors in a manner shown by Figure 3. This led Ashby and Verrall to postulate a diffusional mechanism for this process, also depicted in Figure 3. We note that, unlike grains in a diffusional solid, oil droplets are free to shear in their interiors. Thus the shape changes observed in the grain switching process may not have occurred by diffusional transport as assumed by Ashby and Verrall. The observed deformation may have occurred by viscous flow in the interiors of the droplets. The analog for this kind of deformation in crystalline solids is slip. Thus the grain switching process directly observed by Ashby and Verrall may have involved slip-like processes.

The diffusional model of grain switching has been criticized on the grounds that symmetry is violated in the process envisioned. In the simplest case one imagines a two dimensional array of identical hexagonal grains. The four grains shown in Figure 3(a) would be typical of the initial grain structure. We note that grains 1 and 2 are identical in size and shape

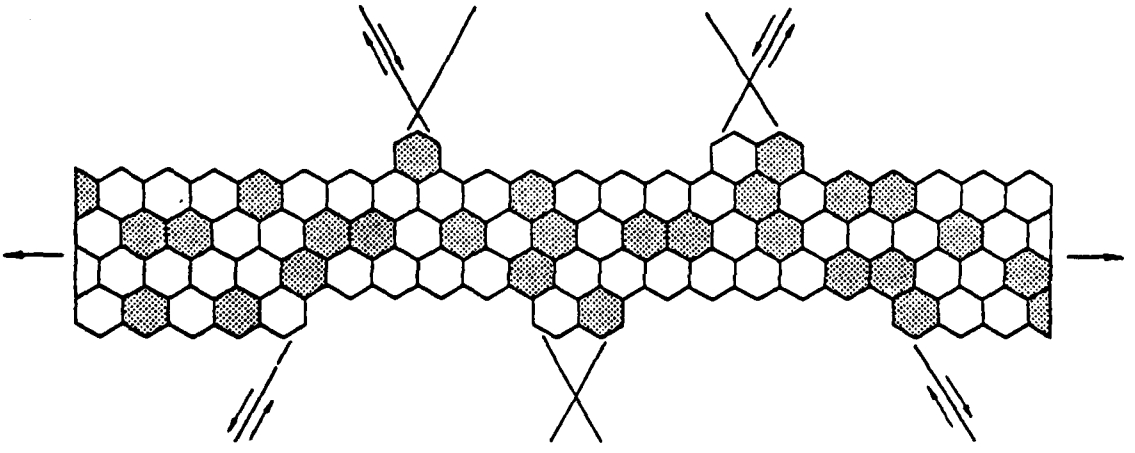

Fig. 2 - Schematic representations of deformation by grain rearrangement. Shading is used to represent two different phases. Shear through the sheet produces "surface grains" as shown

would not qualify as superplastic materials. Similarly, high strain rate sensitivity alone is not sufficient to define superplasticity, since inherent ductility is needed to achieve high elongations. To date all superplastic alloys contain at least one metallic phase, implying that deformability, which is an inherent feature of metals, is required for superplastic flow.

Typical superplastic flow characteristics are shown in Figure 1 for Zn-22%Al [8-9]. The figure shows both steady state flow stress and percentage elongation to failure as a function of imposed strain rate. The log σ-log $\dot{\varepsilon}$ is sigmoidal in nature and is usually divided into three regimes (I, II and III). We note that the maximum elongations to failure coincide with regime II where the strain rate sensitivity, $m=d(\log \sigma)/d(\log \dot{\varepsilon})$, reaches a maximum value. This is expected on the grounds that neck growth is much more gradual when the strain rate sensitivity is high [10].

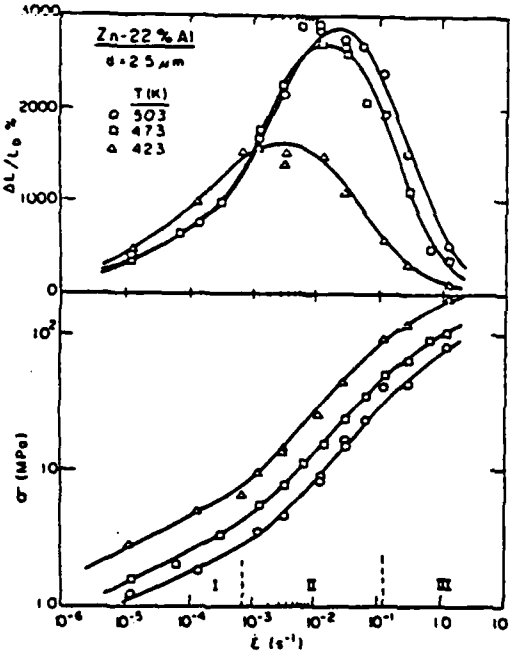

Fig. 1 - Superplastic flow properties of Zn-22%Al [8-9]. (Courtesy of T. G. Langdon)

The three regimes of deformation can be characterized in a number of different ways. The most obvious distinguishing feature is the strain rate sensitivity. Typically the strain rate sensitivity in regime II reaches a maximum value of about 0.5. In regimes I and III it falls to about 0.2, or less for some alloys. Although the log σ-log $\dot{\varepsilon}$ curves appear to be straight in regime II, the corresponding elongation to failure curves show that the maximum elongation occurs at a single strain rate and this implies an inflection point in the stress-strain rate curves.

The three regimes of deformation can also be distinguished by their dependence on temperature and grain size. Typically, activation energies in regimes I and III are large, often about equal to those for lattice self diffusion [11-12]. In regime II smaller activation energies, near those for grain boundary self diffusion are commonly observed [12-13]. When superplasticity is found at high homologous temperatures, as in the case of aluminum alloys, the activation energy for flow in regime II is near that for lattice self diffusion [14].

Deformation in regimes I and II depends strongly on grain size. This grain size dependence is usually expressed in a power law form as $\dot{\varepsilon} \sim d^{-p}$ where the exponent p ranges between 2 and 3 [11-13]. Generally an exponent of p=3 is found at low homologous temperatures whereas p=2 is observed at higher temperatures [14]. These grain size dependencies are similar to those for Coble creep and Nabarro-Herring creep, respectively. Stage III represents a power law creep process and as such does not depend strongly on grain size.

The sigmoidal nature of the curves depends critically on the existence of regime I with a low strain rate sensitivity. This is a controversial aspect of superplastic flow, in part because unambiguous experiments are difficult to conduct in this regime. At low strain rates and long times grain growth can occur. This in turn can cause the strain rate (at a fixed stress) to fall. Such an effect could cause anomalously low strain rate sensitivities to be observed in regime I [15]. Another source of error arises from the difficulty of achieving steady state flow at such low strain rates. In a creep test the strain rate falls markedly with deformation even when the grain size is constant, due to the effects of strain hardening. If the strain rate is measured before steady state is reached, an anomalously high strain rate sensitivity would be found [16]. These opposing errors have been the subject of considerable debate and discussion [16-17]. However, the weight of evidence appears to support the view that the strain rate sensitivity in regime I is indeed low as indicated in Fig. 1 [18], and that the log σ-log $\dot{\varepsilon}$ relation is basically sigmoidal. Many different kinds of fine grained alloys exhibit this kind of behavior.

Superplasticity is characterized by extensive grain boundary sliding and grain rotation. These processes and others allow the grains to remain equiaxed even though the sample as a whole undergoes extensive deformation. Grain boundary sliding itself cannot lead to large strains unless the sliding offsets are accommodated by other processes such as diffusion or crystallographic slip. Just how these accommodating processes occur is the central problem of superplasticity.

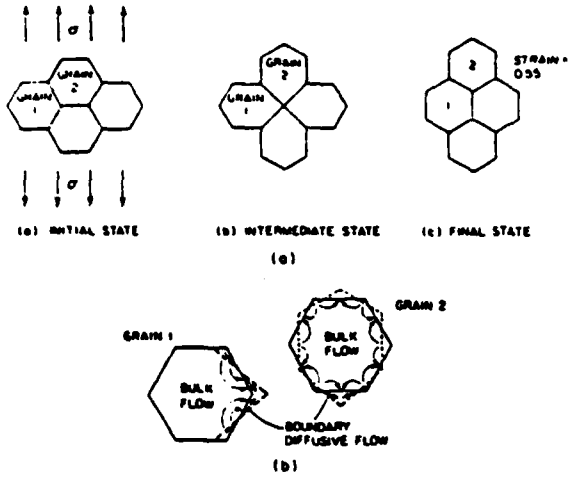

Fig. 3 - A diffusional mechanism for grain rearrangement proposed by Ashby and Verrall [22]

and have identical surroundings. It follows from symmetry that these two grains must deform in the same way. The sequence of grain shapes shown in the figure violates this requirement. Spingarn and Nix [23] have analyzed the suggested diffusional paths in detail and have shown that the Ashby-Verrall process requires grain boundary transport to occur in different directions on opposite sides of the same boundary. If grain boundary diffusion is driven by gradients in normal stresses, as usually assumed, then transport along a boundary cannot be different on either side.

Figure 4 shows the kinds of grain shape changes that would occur if grain boundary sliding and diffusion were the only processes allowed to occur. This process was first described by Lee [24]. Again a perfectly regular array of hexagonal grains is envisioned. We note that each grain deforms in the same way (as required by symmetry) and that the grains simply stretch out during deformation. At a strain of 0.55 triple junctions come together to form an unstable configuration of grain boundaries. For a single phase material new triple junctions would be formed and grain boundary migration would produce the final grain configuration. The final state is the same as that produced by the Ashby-Verrall mechanism. We conclude that the grain switching mechanism proposed by Ashby and Verrall would not occur by grain boundary sliding and diffusion alone and that if these are the only processes allowed, the Lee mechanism would be observed. Furthermore, the kinetics of flow would be the same as for Coble creep under these conditions.

GRAIN ROTATION AND TEXTURE CHANGES - It is well known that grains rotate during superplas-

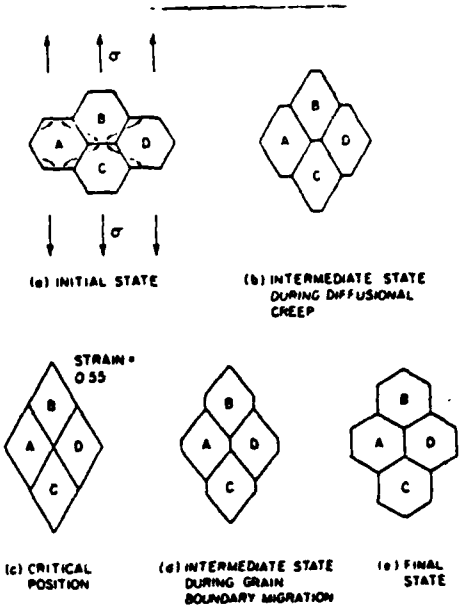

Fig. 4 - Grain shape changes associated with diffusional deformation. The grain switching process involves grain boundary migration [24]

tic flow and that changes in crystallographic texture are produced [25-28]. It is often assumed implicitly that these processes can occur by grain boundary sliding with diffusional accommodation although the need for slip has been recognized by some workers [26-28]. Here we argue that these processes can occur only if slip occurs in some of the grains.

Figure 5 shows the consequences of deforma-

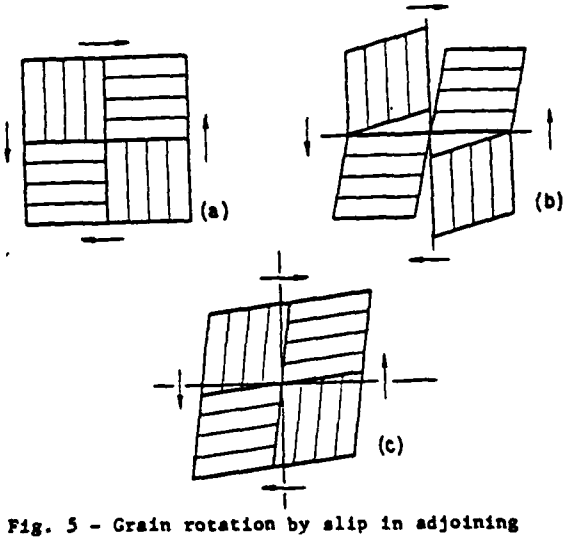

Fig. 5 - Grain rotation by slip in adjoining grains

tion by slip on different planes in different grains. In this simple example a pure shear stress causes each grain to deform by slip on one set of planes. Figure 5(b) shows how the grains would deform if they were isolated from each other. The figure shows that the grains must rotate with respect to each other to maintain compatibility. This is the essence of grain rotation by slip and slip induced changes in crystallographic texture.

As noted above, it is widely assumed that grain rotations can occur as a result of grain boundary sliding and diffusion alone. To investigate this possibility consider the grain shown in Figure 6 which rotates relative to its neighbors. Obviously a simple rotation would create gaps at the grain boundary and would cause some material to overlap as shown. These incompatibilities could be accommodated, however, by diffusional flow along the boundary. We now consider the possible driving forces for this rotation. Clearly such a process would occur spontaneously if an internal moment or torque were applied to the rotating grain. However, in a polycrystalline solid subjected to external forces no such internal moments are present. The motion of any particular grain must be driven by the tractions acting on its boundary. It is possible to show that no net moment acts on a grain subjected to boundary tractions, provided an equilibrium stress state exists within the grain and no internal torques are present [29]. Thus no driving force for grain rotation by diffusional processes exists. We conclude that any grain rotation that occurs must arise from slip within the grains. Since grain rotation is such a central feature of superplasticity, the present observation constitutes a proof that slip must be involved in the superplastic flow process.

It may be possible to account for some grain rotation and changes in texture by grain boundary sliding and diffusion, provided that groups of grains deform and rotate as a whole [30-31]. Consider the grains shown in Figure 7. If sliding is assumed to be easy on the grain boundaries depicted as solid lines and difficult on the dotted boundaries, then each array would deform by anisotropic grain boundary sliding. The shape of each group of grains would be much like the shapes of the individual grains shown in Figure 5 and again compatibility would cause some rotation to occur. However, this model does not explain how individual grains can rotate relative to their neighbors, a feature which is commonly observed in superplasticity.

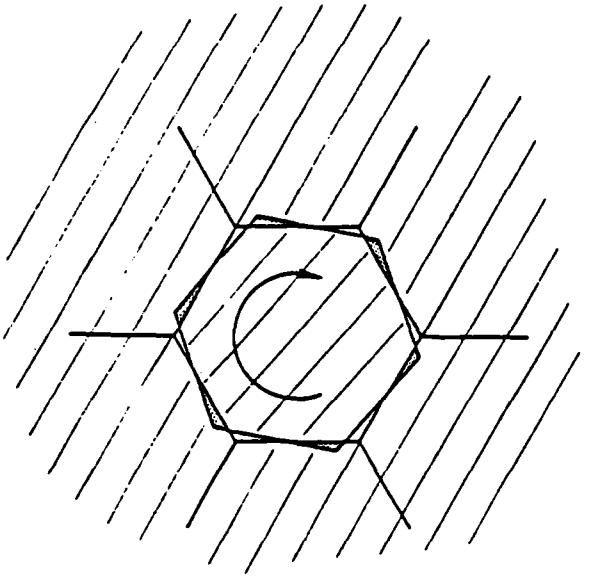

Fig. 6 - Rotation of a grain relative to its neighbors. An internal torque is needed to cause this rotation

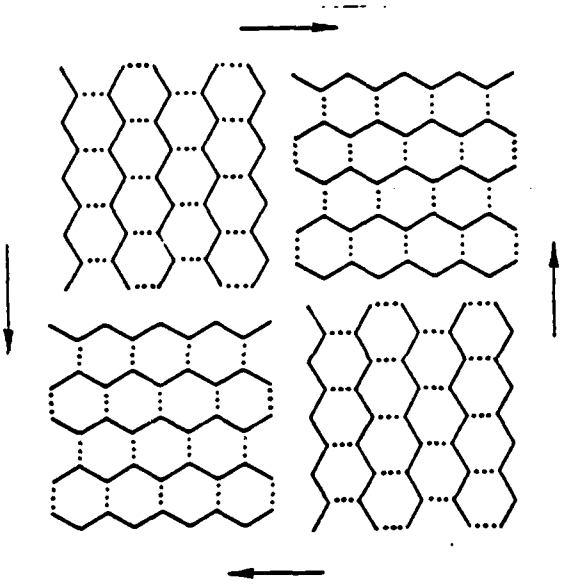

Fig. 7 - Arrays of grains capable of deforming by "anisotropic" grain boundary sliding. Sliding is assumed to be easy on the solid boundaries and difficult on the dotted boundaries

MECHANISMS AND PHENOMENOLOGY OF SUPERPLASTIC FLOW

Most previous approaches to superplasticity have followed one of two different lines of thought. One is based on the assumption of a distinct mechanism for stage II deformation, characterized by $\dot{\epsilon} \sim \sigma^2$. The other is based on the idea that a separate mechanism for superplasticity does not exist and that stage II

deformation is the result of a transition in flow behavior. Models of superplasticity leading to a stress exponent of 2 [32-35] have been criticized on the grounds that elastic singularities associated with dislocation pile-ups (the central feature which leads to the stress exponent of 2) are not stable when grain boundary diffusion is allowed to occur [36]. Indeed, if grain boundary diffusion is allowed to occur naturally, the singularity associated with the pile-up is removed altogether and a linear stress dependence for flow is obtained. As a consequence the various models of superplasticity based on the pile-up, when corrected, do not predict a stress exponent of 2. These are some of the criticisms that have been leveled at the models proposed for stage II deformation. These objections and others become moot if a separate mechanism of superplastic flow does not exist. Below we question the existence of a separate mechanism for stage II flow and claim that the regime of high strain rate sensitivity is the result of a transition in flow behavior involving both slip and diffusion.

Dividing the stress-strain rate curve into three parts as shown in Figure 1 implies the existence of three distinct mechanisms of flow. The shape of the curve places certain restrictions on the flow mechanisms that are of importance in determining the underlying physical processes involved. For example, the mechanisms responsible for regimes II and III must contribute independently to the strain rate since the faster of the two is the controlling process. Two additive processes such as slip and diffusion would satisfy this requirement. Conversely, the mechanisms for regimes I and II must be linked in such a way that the slower of the two controls the strain rate. Grain boundary sliding accommodated by diffusion would satisfy this requirement. In such a description grain boundary sliding itself would have to be slow relative to diffusion in regime I. This is difficult to understand since boundaries which support rapid diffusion would also be expected to slide easily.

Although the extent of regime II is limited by the intervention of regimes I and III, there is no reason in principle why it could not extend over many orders of magnitude of stress and strain rate. However, the regime of maximum strain rate sensitivity at one particular temperature usually extends over a limited range of stress and strain rate, especially if the ductility curves are used as a guide. This implies that the regime of high strain rate sensitivity is merely an inflection point in the log σ-log $\dot{\varepsilon}$ curve and that a separate mechanism for regime II is not required.

Figure 8 shows how sigmoidal stress-strain rate curves at different temperatures could be plotted to reveal an extended regime with a high strain rate sensitivity. We suppose that flow in regimes I and III is controlled by lattice diffusion (with an activation energy Q_L) and that flow in regime II is governed by grain boundary diffusion (with an activation energy $Q_{gb} < Q_L$).

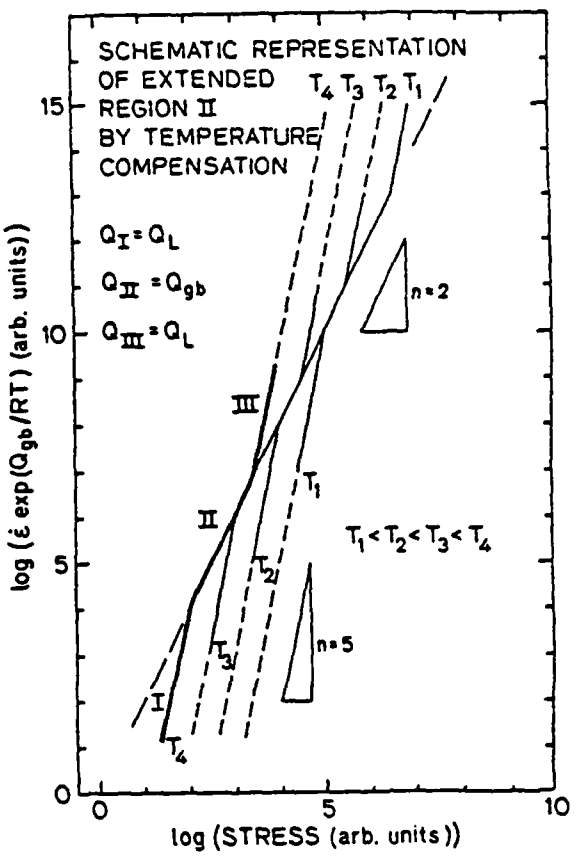

Fig. 8 - Sigmoidal stress-strain relations for a hypothetical superplastic material. Normalization with respect to grain boundary diffusivity causes all of the data for regime II to fall on a common line

When the measured strain rates at different temperatures are normalized with respect to the grain boundary diffusivity, all of the data for regime II fall onto a common curve. In the present example the stress exponent for flow in region II is taken to be 2. By normalizing in this way we obtain a superplastic regime with a strain rate sensitivity of 0.5 (a stress exponent of 2) over 9 orders of magnitude in normalized strain rate. By comparison the extent of regime II at one temperature is limited to three orders of magnitude in strain rate. Figure 9 shows this for the Zn-22%Al data presented in Figure 1. Here the data are plotted in a normalized fashion using an activation energy of 12.1 kcal/mol (50.6 kJ/mol). This normalization does not greatly increase the extent of regime II because the testing temperatures were not widely different. However, the deviations from regime II are clearly evident and they indicate the limited extent of the regime of high strain rate sensitivity. We conclude that the stress-

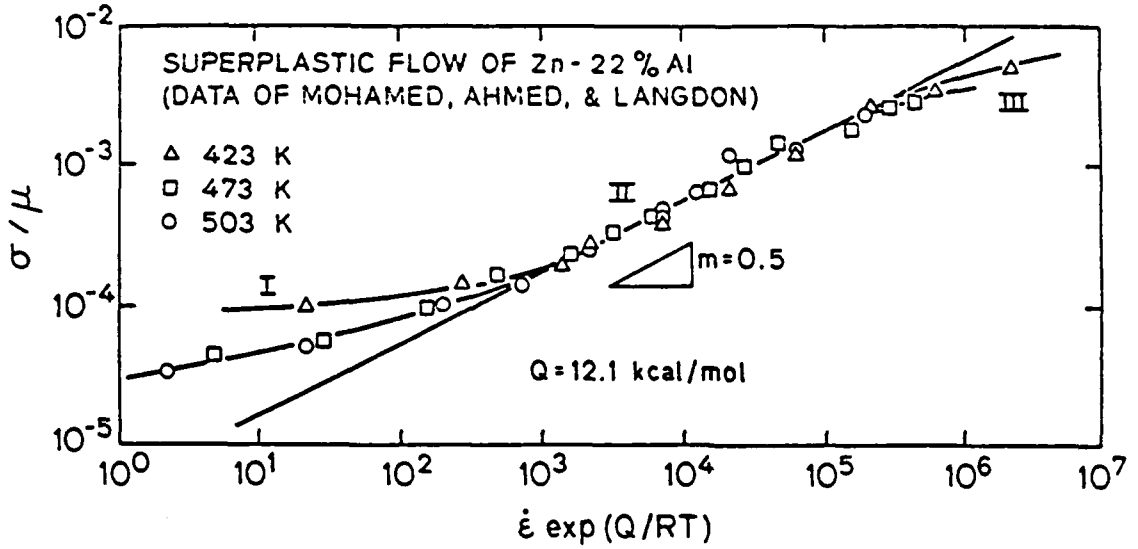

Fig. 9 - Superplastic flow properties of Zn-22%Al plotted in a normalized way. Deviations from a strain rate sensitivity of 0.5 are seen at both high and low strain rates

strain rate relationship is basically sigmoidal in nature and that a separate mechanism is not needed to describe the regime of high strain rate sensitivity.

Although the maximum strain rate sensitivity observed in superplasticity is often about 0.5, this value is not unique. In some cases strain rate sensitivities much greater than 0.5 have been observed. For example, both aluminum and titanium alloys have exhibited strain rate sensitivities as high as 0.9 [3,37]. Also, many materials show superplastic characteristics even when their maximum strain rate sensitivities are less than 0.5. Thus the strain rate sensitivity of 0.5 does not seem to be a unique feature of superplasticity.

Many fine grained metals and alloys exhibit sigmoidal stress-strain rate relations even when they are not classical superplastic materials. This is shown in Figure 10 for a fine grained copper alloy [38]. Here the maximum strain rate sensitivity is about 0.32. Another example is shown in Figure 11 where the steady state flow properties of an oxide dispersion strengthened alloy, MA 754 (essentially Ni-20%Cr containing a fine dispersion of Y_2O_3), are shown for two widely different grain sizes [39-40]. Because of the presence of the oxide dispersion, the stress exponent for flow in the coarse grained material is very high, about 11. Extrapolation of this data to high strain rates appears to coincide with the high strain rate data for the fine grained material. This suggests a sigmoidal relationship for flow of the fine grained material, with a maximum strain rate sensitivity of about 0.30. Like classical superplastic materials, the fine grained MA 754 shows a maximum elongation when the strain rate sensitivity reaches its maximum value. At very low strain rates the strain rate sensitivity is essentially the same as that for the coarse grained material. Here again we see that the presence of fine grains causes a transition in flow behavior to occur. This transition leads to a high strain

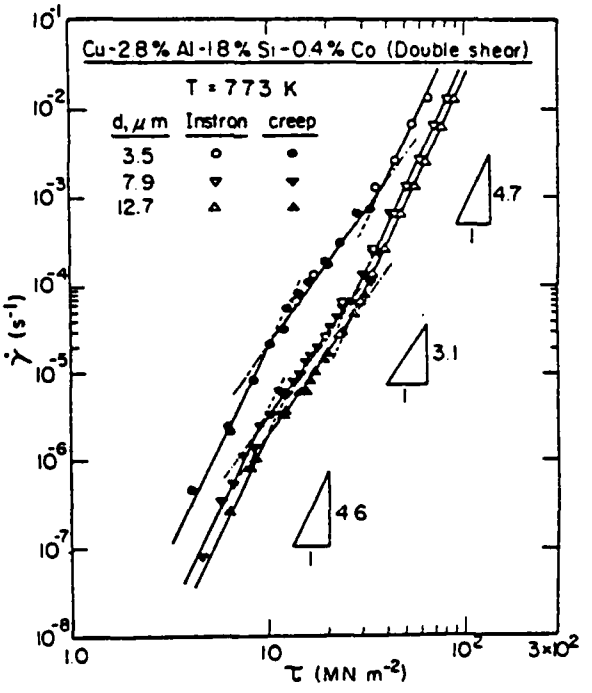

Fig. 10 - Flow properties of a quasi-single phase copper alloy showing superplasticity as a transition in flow behavior [38] (courtesy T. G. Langdon)

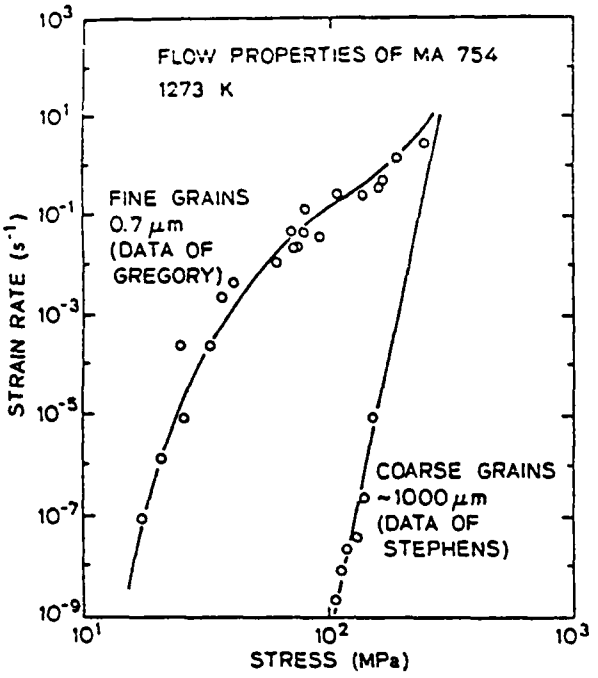

Fig. 11 - Steady state flow properties of MA 754 in both fine grained and coarse grained conditions. A transition in flow behavior is evident in the fine grained data. (Data courtesy of J. K. Gregory [39] and J. J. Stephens [40])

rate sensitivity and high elongation at intermediate strain rates. Again we note that a strain rate sensitivity of 0.5 does not appear to be unique to superplastic flow.

It is interesting to compare the Coble creep rate with the strain rates in the transition regime in Figure 11. For a stress of 100 MPa the Coble creep rate at 1273 K for Ni-20%Cr with a grain size of 0.7 μm is about 10^{-1} s^{-1}. This appears to coincide with the transition and it suggests that the transition in flow behavior is caused by a diffusional relaxation. Further evidence for the role of diffusion in this transition is provided by the observation that the activation energy for flow in this regime is usually the same as that for either grain boundary or lattice diffusion [14]. The observed rate of flow at the lowest stress is at least four orders of magnitude less than the Coble creep rate. This discrepancy suggests that diffusional creep is inhibited at low stresses, although the cause of this inhibition has not been found.

We have seen that the stress-strain rate relationship for many fine grained metals and alloys is sigmoidal in nature and that the regime of high strain rate sensitivity results from a transition in flow behavior caused by a diffusional relaxation. These findings lead naturally to a transitional model for superplasticity which is described in the next section.

TRANSITIONAL MODEL FOR SUPERPLASTICITY

Hart [41] was the first to propose that high strain rate sensitivities leading to superplasticity could be explained as a transition in flow behavior caused by a relaxation process. In his phenomenological treatment, grain boundary sliding was assumed to be the relaxation process which causes a transition in power law creep behavior. Later work by Crossman and Ashby [42] showed that transitions of this kind are extremely narrow. They would be much too narrow to account for superplasticity. More recently this concept was expressed in a different way by Ghosh and Raj [43] who pointed out that transitions in flow behavior would occur naturally in fine grained materials by slip and diffusion if a distribution of grain sizes is present or if the different phases have different diffusional or power law creep properties. This approach, which was studied further by Gregory [44] appears to be an attractive way to account for the sigmoidal nature of the stress-strain rate relations found for fine grained metals.

In the interest of brevity only a brief description of the Ghosh-Raj model is given here. The predictions of the model discussed here are illustrated graphically in Figure 12. We consider the flow properties of an alloy composed of two phases, α and β. Following Ghosh and Raj we assume that both phases deform at the same rate (the overall strain rate) and that the overall stress is given by

$$\sigma = f_\alpha \sigma_\alpha + f_\beta \sigma_\beta$$

where f_α and f_β are the volume fractions and σ_α and σ_β are the flow stresses in the two phases. To make the discussion explicit we assume that $f_\alpha = 0.7$ and $f_\beta = 0.3$. The flow properties of the individual phases are shown by the dashed lines in Figure 12. Each curve shows a power law regime (n = 5) at high stresses and strain rates and a diffusional creep regime (n = 1) at low stresses and strain rates. For purposes of illustration we suppose that when both phases deform by power law creep, the α phase is three times stronger than the β phase (at the same strain rate). Also, we suppose that the grain boundary diffusivities and grain sizes are such that the diffusional creep rate for the α phase is three orders of magnitude faster than that for the β phase.

Under the above assumptions the flow properties of the two phase alloy are given by the solid curve in Figure 12. At very high strain rates both phases deform by power law creep and the overall flow stress falls between that for the two phases. At lower strain rates, diffusional flow begins to occur in the α phase and this causes a transition in the overall flow behavior. At one point in the transition the flow strengths of α and β coincide and are equal to

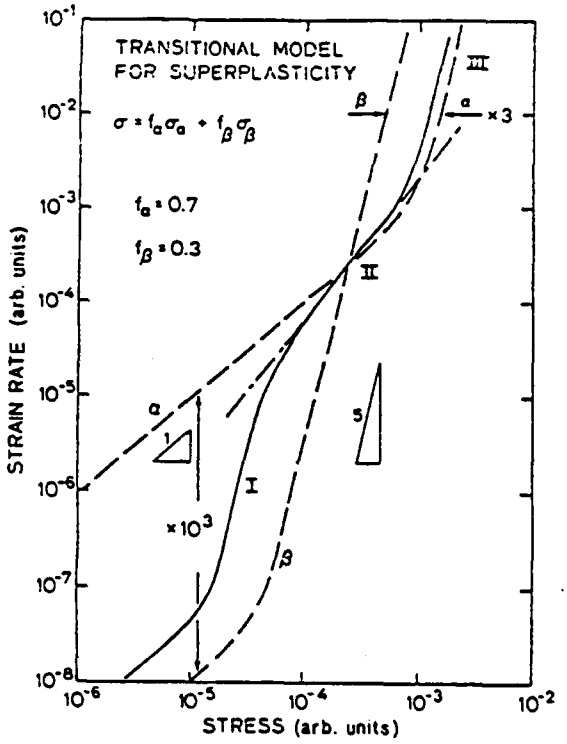

Fig. 12 - Graphical representation of the predictions of the Ghosh-Raj [43] transitional model for superplasticity. The dashed curves represent the flow behavior of the individual phases; the solid curve is the resulting flow behavior of the two phase alloy

the overall flow stress. In the course of this transition the stress within the solid is gradually shifted to the β phase because diffusional relaxation does not permit the α phase to support large stresses. At still lower strain rates virtually all of the stress is supported by the β phase and the deformation is completely determined by flow in that phase.

The result of this diffusional relaxation is a sigmoidal stress-strain rate curve that can be characterized by the three regimes of deformation shown in the figure. It is evident from this that the maximum strain rate sensitivity depends sensitively on the relative strengths and diffusional properties of the two phases and is not a unique value. Since the transition is brought about by a diffusional relaxation, the activation energy for flow in that regime should be the same as that for diffusion. Also, flow in this regime would be strongly dependent on grain size since the diffusional relaxation itself depends on grain size.

In the present treatment diffusional deformation in the β phase would eventually occur at low strain rates. When this occurs the entire solid would exhibit a linear stress dependence for flow. This regime of purely diffusional flow is not observed. This represents one of the major limitations of the transitional model for superplastic flow. At present it is not possible to understand how diffusion could give rise to the transition and not also produce a diffusional deformation regime at low strain rates. This is especially difficult to understand for quasi-single phase alloys in which diffusional flow is inhibited at low stresses and strain rates.

It should be noted that the transitional model for superplastic flow does not indicate how the grain structure remains equiaxed during superplastic flow. This too remains as an unsolved problem.

ACKNOWLEDGMENTS

Discussions with Professor D. M. Barnett regarding the mechanics of solids under surface loading are gratefully acknowledged. This work was supported by the United States Air Force Office of Scientific Research (Grant No. 81-0022) and by the National Science Foundation through the Center for Materials Research at Stanford University.

REFERENCES

1. C. Hammond, in Superplastic Forming of Structural Alloys, Eds. N. E. Paton and C. H. Hamilton, p. 131-145, AIME (1982)

2. D. J. Lloyd and D. M. Moore, in Superplastic Forming of Structural Alloys, Eds. N. E. Paton and C. H. Hamilton, p. 147-172, AIME (1982)

3. C. H. Hamilton, C. C. Bampton and N. E. Paton, in Superplastic Forming of Structural Alloys, Eds. N. E. Paton and C. H. Hamilton, p. 173-189, AIME (1982)

4. N. Ridley, in Superplastic Forming of Structural Alloys, Eds. N. E. Paton and C. H. Hamilton, p. 191-207, AIME (1982)

5. H. F. Merrick, in Superplastic Forming of Structural Alloys, Eds. N. E. Paton and C. H. Hamilton, p. 209-223, AIME (1982)

6. A. F. Giamei, D. L. Anton and R. E. Doiron, in Superplastic Forming of Structural Alloys, Eds. N. E. Paton and C. H. Hamilton, p. 225-239, AIME (1982)

7. O. D. Sherby and O. A. Ruano, in Superplastic Forming of Structural Alloys, Eds. N. E. Paton and C. H. Hamilton, p. 241-254, AIME (1982)

8. H. Ishikawa, F. A. Mohamed and T. G. Langdon, Phil. Mag. 32, 1269-1271 (1975)

9. F. A. Mohamed, M. M. I. Ahmed and T. G. Langdon, Metall. Trans. 8A, 933-938 (1977)

10. T. G. Langdon and D. M. R. Taplin, SM Archives, 2, 329-368 (1977)

11. F. A. Mohamed, S. A. Shei and T. G. Langdon, Acta Metall. 23, 1443-1450 (1975)

12. T. G. Langdon, in Superplastic Forming for Structural Alloys, Eds. N. E. Paton and C. H. Hamilton, p. 27-40, AIME (1982)

13. F. A. Mohamed and T. G. Langdon, Phil. Mag. 32, 697-709 (1975)

14. O. D. Sherby, R. D. Caligiuri, E. S. Kayali and R. A. White, in Advances in Metal Processing (25th Sagamore Army Research Conference), Eds. J. J. Burke, R. Mehrabian and V. Weiss, p. 133-170, Plenum Press (1981)

15. G. Rai and N. J. Grant, Metall. Trans. 6A, 385-390 (1975)

16. D. Grivas, J. W. Morris, Jr. and T. G. Langdon, Scripta Metall. 15, 229-236 (1981)

17. A. Arieli and A. K. Mukherjee, Scripta Metall. 13, 331-338 (1979)

18. S. H. Vale, D. J. Eastgate and P. M. Hazzledine, Scripta Metall. 13, 1157-1162 (1979)

19. D. J. Dingley, Scanning Electron Microscopy/1970, p. 329-336, IIT Research Institute, Chicago (1970)

20. A. E. Geckinli and C. R. Barrett, J. Mater. Sci. 11, 510-521 (1976)

21. D. A. Miller, R. B. Vastava and T. G. Langdon, Microstructural Science 9, 249-256 (1981)

22. M. F. Ashby and R. A. Verrall, Acta Metall. 21, 149-163 (1973).

23. J. R. Spingarn and W. D. Nix, Acta Metall. 26, 1389-1398 (1978)

24. D. Lee, Metall. Trans. 1, 309-311 (1970)

25. J. W. Edington, K. N. Melton and C. P. Cutler, Progress in Materials Science 21, 103-111 (1976)

26. K. Matsuki, K. Minami, M. Tokizawa and Y. Murakami, Metal Sci. 13, 619-626 (1979)

27. K. Matsuki, H. Morita, M. Yamada and Y. Murakami, Metal Sci. 11, 156-163 (1977)

28. K. Matsuki, Y. Uetani, M. Yamada and Y. Murakami, Metal Sci. 10, 235-242 (1976)

29. D. M. Barnett, Stanford University, private communication

30. W. Beere, J. Mater. Sci. 12, 2093-2098 (1977)

31. W. Beere, Phil. Trans. Roy. Soc. (London) A288, 177-196 (1978)

32. A. Ball and M. M. Hutchison, Metal Sci. J. 3, 1-7 (1969).

33. A. K. Mukherjee, Mater. Sci. and Engr. 8, 83-89 (1971)

34. R. C. Gifkins, Metall. Trans. 7A, 1225-1232 (1976)

35. M. Suery and B. Baudelet, Res. Mech. 2, 163-170 (1981)

36. J. R. Spingarn and W. D. Nix, Acta Metall. 27, 171-177 (1979)

37. A. K. Ghosh, in Superplastic Forming of Structural Alloys, Eds. N. E. Paton and C. H. Hamilton, p. 85-103, AIME (1982)

38. S. A. Shei and T. G. Langdon, Acta Metall. 26, 639-646 (1978)

39. J. K. Gregory, J. C. Gibeling and W. D. Nix, submitted to Metall. Trans.

40. J. J. Stephens, Stanford University, unpublished work

41. E. Hart, Acta Metall. 15, 1545-1549 (1967)

42. F. W. Crossman and M. F. Ashby, Acta Metall. 23, 425-440 (1975)

43. A. K. Ghosh and R. Raj, Acta Metall. 29, 607-616 (1981)

44. J. K. Gregory, Ph.D. Dissertation, Stanford University (1983)

III. PUBLICATIONS, REPORTS AND DISSERTATIONS RELATING TO THIS AND PREVIOUS AFOSR GRANTS ON OXIDE DISPERSION STRENGTHENED METALS

A. Publications

1. J. H. Holbrook and W. D. Nix, "Edge Dislocation Climb over Non-Deformable Circular Inclusions", Metall. Trans., 5, 1033 (1974).

2. M. Vikram Rao and W. D. Nix, "Creep in Binary Solid Solutions: A Possible Explanation for Anomalous Behavior", Scripta Met., 7, 1255 (1973).

3. M. A. Burke and W. D. Nix, "Plastic Instabilities in Tension Creep", Acta Met., 23, 793 (1975).

4. R. W. Lund and W. D. Nix, "On High Creep Activation Energies for Dispersion Strengthened Metals", Metall. Trans., 6A, 1329 (1975).

5. R. W. Lund and W. D. Nix, "High Temperature Creep of Ni-20Cr-2ThO_2 Single Crystals", Acta Met., 24, 469 (1976).

6. G. M. Pharr and W. D. Nix, "A Comparison of the Orowan Stress with the Threshold Stress for Creep for Ni-20Cr-2ThO_2 Single Crystals", Scripta Met., 10, 1007 (1976).

7. J. H. Hausselt and W. D. Nix, "Dislocation Structure of Ni-20Cr-2ThO_2 After High Temperature Deformation", Acta Met., 25, 595 (1977).

8. J. H. Hausselt and W. D. Nix, "A Model for High Temperature Deformation of Dispersion Strengthened Metals Based on Substructural Observations in Ni-20Cr-2ThO_2", Acta Met., 25, 1491 (1977).

9. R. F. Singer, W. Blum and W. D. Nix, "The Influence of Second Phase Particles on the Free Dislocation Density During Creep of Stainless Steel", Scripta Met., 14, 755 (1980).

10. R. F. Singer, W. C. Oliver and W. D. Nix, "Identification of Dispersoid Phases Created in Aluminum During Mechanical Alloying", Metall. Trans., 11A, 1895 (1980).

11. P. S. Gilman and W. D. Nix, "The Structure and Properties of Al-Al_2O_3 Alloys Produced by Mechanical Alloying:Powder Processing and Resultant Powder Structures",Metall. Trans. 12A, 813 (1981).

12. W. C. Oliver and W. D. Nix, "The Effects of Strain Hardening in the Hydrostatic Extrusion of Axisymmetric Bi-Metal Rods", Metals Technology, February, 75 (1981).

13. W. D. Nix, "The Effects of Grain Shape on Nabarro-Herring and Coble Creep Processes", Metals Forum, 4, 38 (1981).

14. W. C. Oliver and W. D. Nix, "High Temperature Deformation of Oxide Dispersion Strengthened Al and Al-Mg Solid Solutions", Acta Metall., 30, 1335 (1982).

15. D. M. Barnett, W. C. Oliver and W. D. Nix, "The Binding Force Between and Edge Dislocation and a Fermi-Dirac Solute Atmosphere", Acta Metall., 30, 673 (1982).

16. D. M. Barnett, G. Wong and W. D. Nix, "The Binding Force Between a Peierls-Nabarro Edge Dislocation and a Fermi-Dirac Solute Atmosphere", Acta Metall., 30, 2053 (1982).

17. J. K. Gregory, J. C. Gibeling and W. D. Nix, "High Temperature Deformation of Ultra-Fine-Grained Oxide Dispersion Strengthened Alloys" (to be published in Metall. Trans.).

18. D. J. Srolovitz, M. J. Luton, R. Petkovic-Luton, D. M. Barnett and W. D. Nix, "Diffusionally Modified Dislocation-Particle Elastic Interactions", (to be published in Acta Metall.).

19. J. K. Gregory, J. C. Gibeling and W. D. Nix, "High Temperature Deformation of Extremely Fine Grained MA 754 and MA 6000", Fourth RISØ International Symposium on Metallurgy and Materials Science, Roskilde, Denmark, September, 1983.

20. W. D. Nix, "On Some Fundamental Aspects of Superplastic Flow" (to be published in Proceedings of Superplastic Forming Symposium, 1984).

B. Ph.D. Dissertations

1. R. W. Lund, "A Study of High Temperature Creep of Dispersion Strengthened Ni and Ni-20Cr", Ph.D. Dissertation, Stanford University (1975).

2. J. H. Holbrook, "A Theoretical Investigation of Creep of Dispersion Strengthened Crystals", Ph.D. Dissertation, Stanford University (1976).

3. P. S. Gilman, "The Development of Aluminum-Aluminum Oxide Alloys by Mechanical Alloying", Ph.D. Dissertation, Stanford University (1979).

4. W. C. Oliver, "Strengthening Phases and Deformation Mechanisms in Dispersion Strengthened Solid Solutions and Pure Metals", Ph.D. Dissertation, Stanford University (1981).

5. J. K. Gregory, "Superplastic Deformation in Oxide Dispersion Strengthened Nickel Base Superalloys", Ph.D. Dissertation, Stanford University (1983).

C. Oral Presentations (Speaker Underlined)

1. W. D. Nix, "On the Existence of Steady State Creep", Department of Mechanical Engineering, University of Colorado, Boulder, Colorado (December, 1973).

2. W. D. Nix, "Plastic Instabilities in Tension Creep", Air Force Conference on: Fracture and Fatigue of Two Phase Materials - Effects of Plastic Instability, Fairborn, Ohio (September, 1974).

3. W. D. Nix, "High Temperature Creep of Dispersion Hardened Single Crystals", TMS-AIME (invited paper), University of Toronto (May, 1975).

4. W. D. Nix, "When are Back (Threshold) Stresses Meaningful ?" 1977 Gordon Conference on Physical Metallurgy, Holderness School, Plymouth, N. H., June, 1977. (Invited paper).

5. P. S. Gilman and W. D. Nix, "Mechanical Alloying of Al-Al_2O_3 Alloys", presented at 1978 Spring meeting of AIME in Denver.

6. W. C. Oliver, R. F. Singer and W. D. Nix, "Formation and Identification of Particles in Dispersion Strengthened Aluminum", presented at 1980 Spring Meeting of AIME in Las Vegas.

7. W. C. Oliver, "Mechanical Alloying", presented at Department of Materials Science and Engineering, Industrial Affiliates Meeting at Stanford, June, 1980.

8. W. D. Nix, "Creep of Dispersion Strengthened Metals", presented at EXXON Research Laboratory, Linden, N.J., February, 1980.

9. J. K. Gregory, R. Sinclair and W. D. Nix, "Abnormal Grains in MA753", Annual Meeting of AIME, Chicago, February, 1981.

10. J. K. Gregory, J. C. Gibeling and W. D. Nix, "Superplastic Behavior in MA 6000E", International Symposium on Superplastic Forming of Structured Alloys, San Diego, California, June, 1982.

11. J. K. Gregory and W. D. Nix, "A Model for Superplastic Flow Based on the Coupling of Power Law Creep and Diffusional Deformation", International Symposium on Superplastic Forming of Structural Alloys, San Diego, California, June, 1982 (Poster Session).

12. J. K. Gregory and W. D. Nix, "Flow in an Ultra-Fine Grained Nickel Base Alloy", Poster Session, 1983, Gordon Conference on Physical Metallergy, Holderness School, Plymouth, N.H., June, 1983.

13. J. K. Gregory, J. C. Gibeling and W. D. Nix, "High Temperature Deformation of Extremely Fine Grained MA 754 and MA 6000", Fourth RISØ International Symposium on Metallurgy and Materials Science, Roskilde, Denmark, September, 1983.

14. J. J. Stephens, J. C. Gibeling and W. D. Nix, "Creep and Fracture of MA 754 at Elevated Temperatures", Special Symposium: Physical Metallurgy of High Temperature Alloys, TMS-AIME Fall Meeting, Philadelphia, PA, October, 1983.

IV. PROFESSIONAL PERSONNEL

The following personnel of the Department of Materials Science and Engineering at Stanford have been engaged in this research program:

Principal Investigator:

Dr. William D. Nix, Professor

Senior Research Associate:

Dr. Jeffery C. Gibeling

Graduate Research Assistants:

Ms Jean K. Gregory	B.S.	Massachusetts Inst. of Technology
	M.S.	Stanford University
Mr. John J. Stephens	B.S.	Cornell University
	M.S.	Stevens Institute of Technology
Mr. M. Lufti Ovecoglu	B.S.	Middle East Technical University, Ankara
	M.S.	Middle East Technical University, Ankara